Master's thesis

NTNU
Norwegian University of Science and Technology
Faculty of Engineering
Department of Mechanical and Industrial Engineering

Shah Fahad

Parametric Analysis of the Structural Integrity of a Protective Wall Installed Onboard a Hydrogen Tube Trailer

Master's thesis in Reliability, Availability, Maintainability, and Safety Engineering
Supervisor: Nicola Paltrinieri
Co-supervisor: Cecilia Haskins, Federico Ustolin

June 2021

NTNU
Norwegian University of Science and Technology

Shah Fahad

Parametric Analysis of the Structural Integrity of a Protective Wall Installed Onboard a Hydrogen Tube Trailer

Master's thesis in Reliability, Availability, Maintainability, and Safety Engineering
Supervisor: Nicola Paltrinieri
Co-supervisor: Cecilia Haskins, Federico Ustolin
June 2021

Norwegian University of Science and Technology
Faculty of Engineering
Department of Mechanical and Industrial Engineering

NTNU
Norwegian University of
Science and Technology

Abstract

Hydrogen is a promising candidate for replacing conventional fuels and achieving the greenhouse gaseous emissions target. This has resulted in a greater interest in the development of hydrogen as an energy carrier. Despite advances in the technologies related to hydrogen, safety remains a major concern for hydrogen's social acceptance. Even though there is a body of research to design safety barriers in the case of the catastrophic explosion of hydrogen, there is a lack of research work on the safety of the driver during the transport of hydrogen via trailers even though there are many reported hydrogen-related accidents where the drivers were the first reported casualties.

The objective of the study is to develop consequence-reducing barriers for the loss of containment of compressed gaseous hydrogen (CGH2) in transportation. Due to the theoretical foundation established in the master's specialization report with MCE AS, the company wanted to study further the design of the driver's cabin safety system against the high-pressure blast caused by the loss of CGH2 containment. The study focuses on the design of a novel continuous wall between the driver's cabin and hydrogen storage tanks. The selection of the wall is based on modeling a potential high-impact accident scenario, with pressure shocks against the wall. Then, the options for the construction of the wall are based on the available materials consistent with MCE's technological capabilities, the strength of materials, and allowable wall dimensions. The study evaluates a selection of design considerations for choosing a safety barrier wall, where comparisons are made between the simple barrier wall, reinforced wall, and the pentagonal reinforced barrier. The response to the overpressure effect of the explosion is studied and it is concluded that by using a reinforced pentagonal wall of 50mm thickness, it is possible to safeguard the driver's cabin against the critical event of hydrogen tank explosion.

Sammendrag

Hydrogen er en lovende kandidat for å erstatte konvensjonelle drivstoff og oppnå målet for klimagassutslipp. Dette har resultert i en større interesse for utviklingen av hydrogen som energibærer. Til tross for fremskritt innen teknologiene relatert til hydrogen, er sikkerhet fortsatt en stor bekymring for hydrogens sosiale aksept. Selv om det er en mengde forskning for å designe sikkerhetsbarrierer i tilfelle den katastrofale eksplosjonen av hydrogen, mangler det forskningsarbeid om førerens sikkerhet under transport av hydrogen via tilhengere, selv om det er mange rapporterte hydrogen- relaterte ulykker der sjåførene var de første rapporterte omkomne.

Målet med studien er å utvikle konsekvensreduserende barrierer for tap av inneslutning av komprimert gassformig hydrogen (CGH2) under transport. På grunn av det teoretiske grunnlaget som ble etablert i masterns spesialiseringsrapport med MCE AS, ønsket selskapet å studere videre utformingen av førerhusets sikkerhetssystem mot høytrykkssprengning forårsaket av tap av CGH2-inneslutning. Studien fokuserer på utformingen av en ny kontinuerlig vegg mellom førerhuset og lagringstankene for hydrogen. Valget av veggen er basert på modellering av et potensielt storeffektulykkesscenario, med trykkstøt mot veggen. Deretter er alternativene for konstruksjon av veggen basert på tilgjengelige materialer i samsvar med MCEs teknologiske evner, styrken på materialene og tillatte veggdimensjoner. Studien evaluerer et utvalg av designhensyn for valg av sikkerhetsbarrierevegg, der sammenligninger blir gjort mellom den enkle barriereveggen, den forsterkede veggen og den femkantede armerte barrieren. Responsen på eksplosjonens overtrykkeffekt studeres og det konkluderes med at det ved hjelp av en forsterket femkantet vegg med en tykkelse på 50 mm er mulig å beskytte førerhuset mot den kritiske hendelsen av hydrogentankeksplosjon.

Preface

The master's thesis is the mandatory part of the two-year international master's degree program in Reliability, Availability, Maintainability, and Safety (RAMS) Engineering at the Norwegian University of Science and Engineering (NTNU). The thesis is carried out in collaboration with the company, MCE AS during the spring semester of 2021.

Acknowledgment

I would like to extend my gratitude towards my supervisor Nicola Paltrinieri for his invaluable support and directions. I would like to say thanks to Cecilia Haskins as my co-supervisor for collaboration with all stakeholders and useful inputs throughout the thesis. I would like to acknowledge my co-supervisor, Federico Ustolin for his mentorship and constant technical guidance throughout the modeling and writing phases of the thesis. I would also extend my thanks to Eldar Tranøy, the CEO of MCE AS for his engagement, counseling, and collaboration alongside his other commitments.

Contents

Table of figures

List of Tables

Acronyms and Definitions

ADR	European Agreement concerning the International Carriage of Dangerous Goods by Road
ARAMIS	Accidental Risk Assessment Methodology for Industries
ATR	Autothermal reforming
BLEVE	Boiling Liquid Expanding Vapor Explosion
CCGH2	Cryo-Compressed Hydrogen
CGH2	Compressed gaseous hydrogen
CCS	Carbon Capture and Storage
CE	Critical Event
CFD	Computational Fluid Dynamics
CGH2	Compressed Gaseous Hydrogen
GHG	Greenhouse gases
GHS	Globally Harmonized System of Classification and Labelling of Chemicals
LH2	Liquified or liquid hydrogen
LOC	Loss of containment
LPI	Loss of physical integrity
MLI	Multi-layered Insulation
NTP	Normal temperature and pressure; (293.15K, 101.325kPa)
RPT	Rapid phase transition
SMR	Steam reforming of methane
VCE	Vapor cloud explosion
Cryogenics	Corresponding to temperatures less than 120 K
Deflagration	Deflagration is the propagation of a combustion zone at a velocity less than the speed of sound in the unreacted mixture.
Detonation	Detonation is the propagation of a combustion zone at a velocity greater than the speed of sound in the unreacted mixture.
Explosion	The sudden release of a large amount of energy generating a blast wave.
Overpressure	Overpressure is blast wave pressure above the atmospheric pressure or the pressure in a containment structure above the atmospheric pressure

1. Introduction

1.1 Hydrogen Overview

Hydrogen is the lightest element with a standard atomic weight of 1.008 AMU (atomic mass units) and is the most abundant substance in the universe (Zohuri, 2019). Hydrogen is one of the most promising energy carriers, with several advantages to be used in the transportation, heating, and power generation sectors. With the world energy production shifting focus towards green and renewable energies, the significance of hydrogen cannot be ignored, as it is a potentially clean and renewable energy carrier, non-toxic, with a high gravimetric energy content (Zohuri, 2019). Several studies and projects of all the phases of the life cycle have been carried out by the world major economies, including the European Union, Australia, Germany, and Japan (Michel et al., 2021)

Even though hydrogen has several advantages compared to conventional energy carriers, a few drawbacks must be tackled. For instance, it is still more expensive than hydrocarbons (Rostrup-Nielsen and Rostrup-Nielsen, 2002), has storage and transportation issues, and a knowledge gap on the loss of integrity of its storage equipment is still present (Ustolin et al., 2020). Although it is evident that hydrogen has both pros and cons to replace conventional fuels, the issues with hydrogen are deemed solvable. This is evident from the enormous amount of interest shown by the big companies and the research institutions and is considered a key player towards zero-carbon energy system(Rosen and Koohi-Fayegh, 2016).

1.2 Project Description and Problem formulation

The focus of this thesis is the safety of compressed gaseous hydrogen (CGH2) in transportation. With a theoretical background established in the specialization thesis, the company MCE AS was interested in the safer design of tanks, based on their technical capabilities and research interests. Since the company is interested in hydrogen transportation, the safety of the driver's cabin in case of loss of containment of CGH2 was a key area of concern for them. By reviewing safety assessment techniques and focusing on the right side of the bowtie diagram, an attempt is being made to reduce the implications of the hazardous event. The study of the effects of consequence-reducing barriers (mainly protective walls) for CGH2 loss of containment is useful for the transportation regulations and installation standards.

1.2.1 Motivation and Objectives

The motivation of the thesis comes from the recent overwhelming interest of the Norwegian government (Norwegian Ministry of Petroleum and Energy, 2020) and the private sector in adapting alternate green technologies as a replacement for conventional fossil fuels, as this is reflected from the interest by MCE AS in their interest in research within hydrogen technologies. After the master's project was carried out in collaboration with the Norwegian company, MCE AS, the company wanted a further detailed safety analysis of the storage technologies. Based on the findings of the specialization report, the company found itself more suited to use CGH2 for its hydrogen transportation business. The goal of the study is to provide overall hazards through comprehensive risk assessment techniques. The study involves a thorough structural analysis by using a finite element method, to ensure the safest possible configurations of safety wall, for both ignited and non-ignited loss of containment.

MCE AS is a Norwegian company with its workshop located at Etne municipality. MCE has broad expertise in dealing with engineering materials for the construction of large vehicles' bodywork, production, installation of steel structures, and a distributor of industrial gases. Moreover, the company plans to contribute to the clean energy market and intends to add the transportation of hydrogen to its industrial gas distribution business(MCE, 2021). For the thesis, the company wanted primarily to explore the design options related to the driver's cabin safety, in addition to the overview on storage technologies. As the focus of the study is the safety of the road transportation of CGH2, according to ADR section 9.3.3, the driver's compartment shall be separated from the load compartment by a continuous wall

In the following the main objectives of the thesis are listed:

- Design of the boundary wall between the tank and the driver's cabin to mitigate the consequences of the critical event (explosion) over the driver's chamber.
- Analysis of the required physical and mechanical properties for the boundary wall, and suggestion of additional layers of protection to MCE AS
- To provide support for the risk assessment and safety design for CGH2 transportation through roads

1.2.2 Project Scope and Limitations

The focus of the thesis is limited to the design of the continuous wall between the driver's cabin and the CGH2 (Compressed gaseous hydrogen) tanks. The study is aimed at focusing on CGH2 transport. However, the bias towards using gaseous hydrogen transport on Norwegian road transport is since the compressed gaseous hydrogen transport was concluded to be more suited to their business needs. While the study focuses on the design of the wall, an additional layer of protection (Fire protection coating) against the loss of containment has been mentioned, but due to the limited amount of data for modeling, the overall effect on cabin safety has not been modeled.

1.3 Structure

The rest of the study follows the following structure. Chapter 2 focuses on the theoretical foundations used for the literature review. It addresses research questions based on the gaps uncovered in the background. Chapter 3 discusses the methods and tools used to structure the research. The chapter discusses in detail the methods, and tools, their limitations, and their validity. Chapter 4 discusses the empirical results. Chapter 5 discusses how the findings relate to the support of our objectives of the thesis answers. Chapter 6 shares insights and ideas for what remains to be done in the research, which is followed by the references and appendix.

2. Background

2.1 Hydrogen as the alternative energy carrier

Hydrogen has a good potential to replace conventional fuels to fulfill the world's ever-increasing energy demand and to cut the overall hazardous emissions. According to (Pant and Gupta, 2009), hydrogen has high energy content per unit of mass (140 MJ/kg) in comparison with gasoline (48.6 MJ/kg). Hydrogen can be considered a low or zero-emission energy carrier if the methods of production utilize non-fossil fuels such as biomass, organic matter, water electrolysis, etc (Ustolin et al., 2020, Zeng and Zhang, 2010) but the production from fossil fuels subsequently require carbon separation techniques for it to be a clean method.

Hydrogen must be safe and accessible to be a viable alternative energy source. It must be compressed to increase its energy density and improve storage and transport efficiency. The challenges for using hydrogen as an energy carrier vary with the state of the hydrogen (e.g. gaseous or liquid) being used for storage and transportation. The choice of the state of hydrogen is subject to several factors like storage capacities, demand volumes, and transport distances, etc (Yang and Ogden, 2007). Pressurized hydrogen can be transported in gas tanks on trucks, ships, and trains. Pipeline transport is a viable transporting medium for long distances. For very long distances, LH2 is a more suited transportation method(Yang and Ogden, 2007). Since the liquefaction of hydrogen is a costly process compared to the compression one, LH2 is usually more suited for longer distances and moderate demands. (Lahnaoui et al., 2018).

In Norway, the lack of access to LH2 is a huge barrier in hydrogen to replace other fuels due to high liquefication costs (CleanTech, 2019). Economically, LH2 is not competitive with other fuels and currently, any demand in Norway for LH2 must be met by imports (CleanTech, 2019). This requires the usage of cryogenic tanks on trucks for road transport or through ferries by sea. Equinor holds 2023 as the best-case scenario for production at the industrial facility in Møre og Romsdal county, Tjeldbergodden, but with 2025 as a more realistic estimate for the production (Øystese, 2019). An increase in Hydrogen production is key to reduce the costs for liquefaction and make the prices competitive. With a tenfold increase in the production capacity, the energy needed for liquefaction can be reduced by 50 % (CleanTech, 2019). The European Agreement concerning the International Carriage of Dangerous Goods by Road (ADR) directive provides regulation for transport by truck in addition to regulations related to the container systems. Hydrogen is subjected to the ADR regulations in the transportation of dangerous goods.

2.2 Hydrogen in Norway

Norway is a major natural gas producer, with large hydropower resources and recent developments in offshore wind projects, thereby giving Norway a huge potential to be an exporter of clean hydrogen in the future. Low carbon hydrogen can be abundantly produced in Northern Norway as it has huge renewable energy and natural gas reserves which can be converted into low carbon hydrogen. The Norwegian domestic electric energy is 96% covered by the current local hydropower infrastructure and is actively involved in significantly increasing wind power (Aleixo et al., 2012). Since the Norwegian coastline is quite extended (100,915 km(Environment, 2021) and is well suited for offshore wind installations, the study carried out by Norway's concludes the huge potential of hydrogen in Norway, especially in the transport sector (HyWays, 2008). However, ammonia, as H2 based energy carriers as per study based on the cost, energy efficiency, and CO2 footprint (Ishimoto et al., 2020) compare the

Levelized cost of LH2, and ammonia delivered from Norway to Rotterdam to be of the range 5.0 EUR/kg-H2, which in comparison to NH3 is less (7 EUR/kg-H2). (Andreassen et al., 1993) reviewed hydrogen production with 100 MW hydropower input via electrolysis for transporting from Norway to Germany via LH2 tanks in ships and ISO containers. The capacity was estimated to be only 500 tons per day. (Stiller et al., 2008) carried out a similar study and analyzed hydrogen production and transport from Norway to Germany employing pipelines from the North sea to the European continent.

According to the study carried out by (HyWays, 2008), Norway with its sparse road networks, (e.g. Oslo-Grenland via E18, Grenland-Stavanger via E18/39, and Stavanger-Bergen via E39) shall be equipped with hydrogen fuelling stations to facilitate the early users of hydrogen fuel via road. According to (Damman et al., 2020), land transport is a potential market, and there are government initiatives and incentives. However, this sector has not been the main or the solely focused sector for hydrogen applications. Given the fact that the emissions in the maritime sector are expected to account for 17% of global emissions, and that Norway itself had emissions of 7.4 million tonnes, and is expected to further increase to 11.5 million tonnes by 2040, hydrogen and ammonia are key candidates to reach the 2050 emissions cut from the maritime sector by 50% (Damman et al., 2020). Norway has shifted its focus on hydrogen in the maritime sector, as it was evident from at least 10 pilot projects on hydrogen-fuelled ships shortly. The development of Pilot-E as a large support scheme to facilitate green shipping solutions by the Norwegian government also indicates the significance of hydrogen in the maritime industry. In addition, hydrogen is great potential in the industry sector. In the industry sector, Yara has launched green fertilizers production where they see hydrogen as a key player in achieving the green shift.

2.3 Hydrogen Lifecycle

2.3.1 Production

Hydrogen is already being used in several applications, mainly as a feedstock in various industrial applications, ranging from refineries to ammonia and methanol producing industries (Michel et al., 2021). The global demand is ever increasing, as the figures show a spike from 20 Mt in 1975 to approximately 70 Mt in 2018 (IEA (2019)). Today, a strong consensus has been built upon the potential in hydrogen to address the clean energy crisis, and in a recovery perspective to the ongoing COVID 19 pandemic. Based on production technologies, hydrogen has been color-coded as follows (Michel et al., 2021, Newborough and Cooley, 2020)

- Grey hydrogen, being produced from fossil fuels (mainly natural gas and coal) and is causing pollution in the form of emissions of Carbon dioxide gases.
- Blue hydrogen, being produced from conventional fuels like grey hydrogen, but further processed with carbon capture and sequestration (CCS) technique to reduce GHG emissions.
- Green hydrogen, being produced from electrolysis, mainly with the supply of clean renewable electricity.
- Yellow hydrogen, being produced by electrolyzers supplied by the power generated from nuclear plants.
- Turquoise hydrogen, being produced from the fossil fuel's pyrolysis and results in the by-product as solid carbon.

Alternate nomenclatures in addition to these color codes are also popular when referring to hydrogen pathways, e.g "clean hydrogen", "low carbon hydrogen", however, there is no clear standard to give a common reference. To give an overview of pathways, figure 1 gives a good illustration based on the five-color codes as described above.

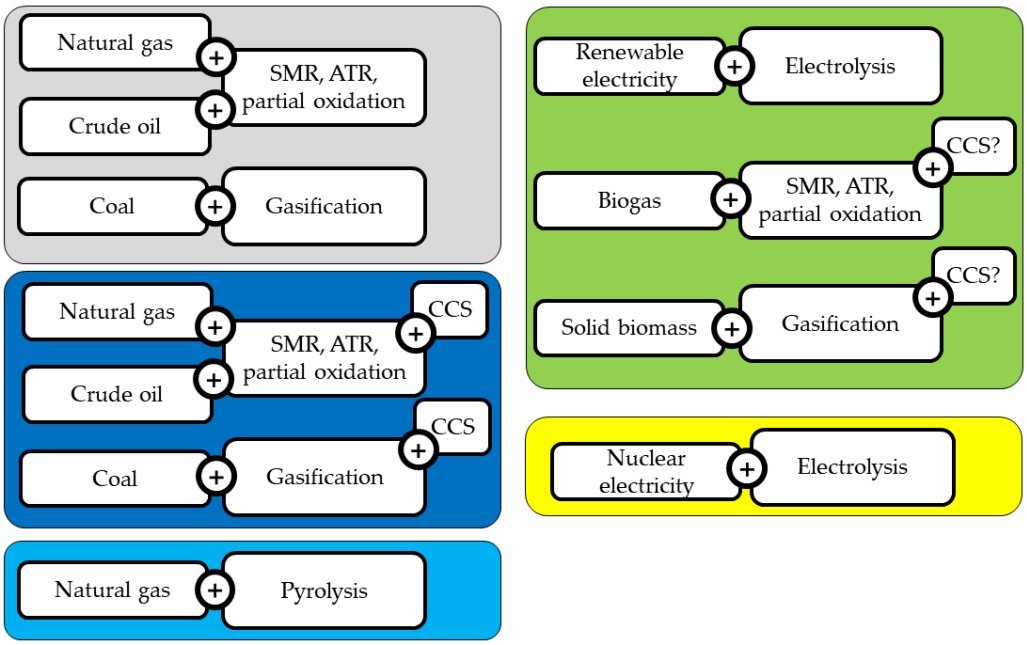

Figure 1: Hydrogen pathways divided by color codes (Adapted from (Newborough and Cooley, 2020)

2.3.2 Storage

Hydrogen needs to be stored safely at different levels of its supply chain, depending on the physical state of hydrogen, volume, duration of storage, and other operational parameters. Due to the low density of hydrogen, its storage requires special attention, and in most cases, it poses a limitation on the amount of hydrogen. In its supply chain, hydrogen needs to be stored at terminals, refueling stations, vehicles like cars, trucks, and ships. Essentially, there are four types of vessels, depending on the material of the containment vessels and affecting the cost, weight, volume, and selection of the state of the hydrogen. These are named types I, II, III, and IV. The type IV tanks offer a maximum allowable pressure of up to 100 MPa (Barthelemy et al., 2017). For compressed gaseous hydrogen, generally operating pressures range from 50-100 MPa in these storage vessels (Newborough and Cooley, 2020).

Hydrogen can also be stored in a liquid state. However, this mode of storage can only pay off when hydrogen is already available in the liquid state since liquefaction of hydrogen is highly costly. For liquefaction of hydrogen, the power consumption per kg is 12.5-15 KWh (Bracha et al., 1994), however technological improvements can significantly reduce the costs related to energy consumption for this mode of storage to economically viable. Liquid hydrogen has the drawbacks of its boil-offs, (Newborough and Cooley, 2020). This is a major safety concern as the evaporation can create the potential loss of containment. Several solutions have been proposed to limit the boil-off, e.g the usage of additional refrigeration systems, vacuum installation, and liquid nitrogen cooling (Wijayanta et al., 2019).

Another option for hydrogen storage is the possibility of using absorbent materials to decrease the storage pressure of gaseous hydrogen. As such, solid-state hydrogen storage materials are classified into metal hydrides, and porous materials. The hydrides store hydrogen chemically via bonding, whereas the porous materials use the physical absorption method (Crow, 2019). LOHC (Liquid organic hydrogen carriers) offers a lot of promise in offering advantages over conventional storage systems. (Modisha et al., 2019). LOHC involves the bonding of hydrogen to liquid carriers by hydrogenation.

The cyclic hydrogenation and dehydrogenation can be used for storing and using on-demand, where the liquid carrier itself is never consumed in the process (Templier and Paré, 2015).

Table 1: Six basic hydrogen storage methods. RT stands for room temperature (25°C) adapted from (Züttel, 2004)

Storage Methods	**Gravimetric density (apprx mass %)**	**Volumetric density (kg H_2 m^{-3})**	**Temperature (K)**	**Pressure (bar)**	**Remarks**
High-pressure gas cylinders	13	<40	RT	800	Usually used in lightweight composite cylinders
Liquid hydrogen in cryogenic tanks	Size dependent	70.8	-252	1	LH2, at RT, continuous loss of hydrogen per day is an issue
Adsorbed hydrogen	2	20	-80	100	Fully reversible physisorption
Complex compounds	<18	150	>100	1	Adsorption at elevated temperature
Oxidation of Metals	<40	>150	RT	1	Chemical oxidation of metal with water, and hydrogen liberation
Absorbed on interstitial sites in host metal	2	150	RT	1	Hydrogen intercalation in host metals

2.4 Hydrogen Properties and Safety

2.4.1 Hydrogen Properties

Hydrogen is highly flammable, and the fact that hydrogen is quite light in gaseous form means that in case of loss of containment, it will quickly rise and disperse in the air before ignition unless the escape of gas occurs in a confined space. Hydrogen does not naturally occur as a gas on earth but is usually found in combination with other elements. It is colorless, odorless, non-toxic, and accounts for 75% of the mass of the universe (Momirlan and Veziroglu, 2005). At atmospheric conditions, it is a diatomic gas with extremely low density (0.0838 kg/m^3) (McCarty et al., 1981). Hydrogen has higher specific energy (119.93 MJ/kg) (Bossel and Eliasson, 2003), in comparison to LNG (50.0 MJ/kg) and gasoline (47.4 MJ/kg) (Veziro and Barbir, 1992).

Table 2: Properties of hydrogen in comparison with gasoline ((Das, 1990), (White et al., 2006), (Pant and Gupta, 2009))

Properties	**Hydrogen**	**Gasoline**
Density (kg/m^3)	0.08987	730
Minimum Ignition energy (mJ)	0.02	0.24
Flame Velocity (m/s)	1.85	0.37-0.43
Autoignition energy temperature in air (K)	858	550
Heat of Combustion (MJ/kgair)	3.37	2.83
Flammability Limits (Φ)	0.1-7.1	0.7-4.0

Table 2 shows the comparison of some selective properties of hydrogen with gasoline at normal temperature and pressure (NTP). The properties like high heat of combustion, high flammability limits,

and low minimum ignition energy for hydrogen gas in a controlled environment can make it a favorable choice as fuel, but the safety of hydrogen is a major concern. These chemical properties make hydrogen an extremely aggressive gas, and the fact that it has extremely low ignition energy, any unchecked sparks or ignition hazards must be considered in hydrogen applications. Some of the major hydrogen storage and transport-related accidents have been mentioned in the next subsection.

2.4.2 Fire, Detonation, and Deflagration

Fire is a non-explosive, combustion of an air-fuel mixture. In the event of a fire, the flame is relatively stationary where the combustible material and air gradually diffuses into the combustion zone (Cadwallader and Herring, 1999). The flame of fire would release an equal amount of energy as compared to the deflagration event, the difference is only in the slower release rate for fire. Hydrogen fire burns without smoke, however it is a safety hazard and can threaten life or property via smoke inhalation (if hydrogen ignites with other combustible materials), and heat exposure. Hydrogen jet fires, which are diffusion flames, are caused by hydrogen loss of containment off pressurized vessels. They are although hazardous, but their overpressures are not as huge as deflagrations. Since hydrogen has one of the lowest ignition energies, and a wide flammability limit, it is very rare for hydrogen to have a “no fire” gas cloud release scenario. Deflagration is also the combustion of an air-fuel mixture, where the combustion propagation is subsonic (<350m/s). According to(Cadwallader and Herring, 1999), deflagration is a rather modest energy release event, and the typical overpressures would rarely exceed the eight times of the initial pressure, generally quite lower than this maximum overpressure. Hydrogen flame speed is generally much higher than the flame velocity, as the combustion causes the flam front to be pushed ahead via the expanding due to burnt gases. This would cause both the velocity and temperature of the combustion wave to increase, thereby resulting in the increased concentration, which serves as a basis for energy release. Theoretically, the overpressure generated is much lesser than the theoretical maximum of 8:1 (Cadwallader and Herring, 1999). A transition to detonation is also possible, subject to several factors like the degree of confinement, obstacles, ignition sources, weather condition, humidity, and wind, etc (Cadwallader and Herring, 1999).

Detonation is the combustion of an air-fuel mixture where the combustion propagates at supersonic speed. Detonation happens faster than deflagration and results in higher combustion energy outputs. A prerequisite for it to happen is to have a high energy ignitor, of the ranges 10 Kj or greater and would result in a high energy blast wave. The overpressure will have a value of the range 14:1, whereas 1 is the pressure in case the cloud was directly ignited (Cadwallader and Herring, 1999). A major problem with detonation is the detonation shock waves, resulting in the formation of detonation cells (reflections of the shock waves, thus resulting in reacting with the primary shock wave and forming complicated Mach stem shock waves).

2.4.3 Hydrogen Major Accidents

In the following, some key hydrogen transport and storage-related accidents, which indicate a high level of safety assessment, design of barriers, and emergency preparedness are reported.

In January 2007, a hydrogen delivery-related accident was reported at Muskingum River Coal Plant, that caused critical damage and resulted in one fatality and 10 injuries (Neville, 2009). The accident killed the truck driver. The root cause points to one of the relief valve rupture disc premature failure.

Another incident involving hydrogen transport was in California in February 2018 where a truck that was carrying 25 composites, carbon fiber, aluminum lined cylinders resulted in a fire. Even though no casualties were reported, the incident resulted in evacuating about 1500-2000 people in the vicinity

(Barilo et al., 2019). The RCA(root cause analysis) identified several incorrectly installed Pressure relief devices (PRDS), and incorrect compression fitting and tubing in addition to other safety gaps.

In 2019, the Uno-X fuel station in Kjørbo, Norway experienced an accident, due to an assembly error of a specialized plugin high-pressure hydrogen storage tank as indicated by the study carried out by GEXCON. In 2020, in Taiwan, a hydrogen tanker crash resulted in an explosion that killed the driver.

2.5 Hydrogen Damage (HD) and Choice of Materials

Hydrogen can significantly deteriorate the physical properties of metals. Hydrogen damages (HD) is referred to as the phenomenon by which the properties of hydrogen affect the materials used in the containment of hydrogen vessels (Ustolin et al., 2020). In Table 3, three main factors induce the HD phenomenon: materials, source of hydrogen, and operating conditions.

The largest category of HD is hydrogen embrittlement (HE). It can be in the form of hydrogen environment embrittlement (HE), hydrogen stress cracking (HSC), and loss in tensile ductility. According to the usual source of hydrogen is gaseous. According to (Edeskuty and Stewart, 1996) this could be in the form of Hydrogen Reaction Embrittlement, in which hydrogen chemically combines the constituents of metals, Internal Hydrogen Embrittlement, in which hydrogen in metal processing gets induced, whereas Environmental Hydrogen Embrittlement results when hydrogen in the atmosphere is reacted with the meta. HE must be avoided by considering the design and choosing the materials and atmosphere that are less likely to react with the metals. As such, welds are the hotspots for HE, where the welded areas produce hard spots, residual stresses, and the microstructure that is conducive to embrittlement (Edeskuty and Stewart, 1996)

Table 3: Hydrogen embrittlement (Adapted from (Hirth and Johnson, 1976))

	Hydrogen environment embrittlement	**Hydrogen stress cracking**	**Loss in tensile ductility**	**Hydrogen attack**	**Blistering**	**Shatter cracks, flakes, fisheyes**	**Micro-perforation**	**Degradation in flow properties**	**Metal hydride formation**
Materials	Steels, Ni-base alloys, metastable stainless steel, Ti alloys	Carbon and low alloy steels	Steels, Ni-base alloys, Be-Cu bronze, Al alloys	Carbon and low alloy steels	Steel, Cu, Al	Steels (forgings and castings)	Steels (compressor)	Fe, steels, Ni-base alloys	V, Nb, Ta, Ti, Zr, U
Source of hydrogen	CGH2	Thermal processing, electrolysis, corrosion	CGH2, internal hydrogen from electrochemical charging	CGH2	H_2S corrosion, electrolytic charging, CGH2	Water vapor reacting with molten steel	CGH2	CGH2 or internal H_2	Internal H2 frommelt; corrosion, electrolyte charging welding
Conditions	$10^{-12} \div 10^2$ MPa, -100 ÷ 700 °C	0.1 ÷ 10 ppm H_2 content, -100 ÷ 100 °C	0.1 ÷ 10 ppm H_2 content, -100 ÷ 100 °C	Up to 10^2 MPa at 200 ÷ 595 °C	H_2 activity 0.2 ÷ 1 x 10^2 MPa at 200 ÷ 595 °C	Precipitation of dissolved ingot cooling	$2 \div 8 \times 10^6$ MPa at 20 ÷ 100 °C<	1 ÷ 10 ppm H^2 content, up to 10^2 MPa	$0.1 \div 10^2$ MPa

2.6 Hydrogen Regulations and standards

2.6.1 ISO Standards

Since there is a lack of national and EU regulations for the handling of hydrogen fuel in several innovative applications such as in the maritime field (ref), International standards must be followed in the design of safe containers to reduce to the minimum, the loss of integrity (LOI). At the international level, ISO Technical committee 197 takes care of developing standards related to 10 hydrogen applications (Gerboni 2016). ISO 17519 standard has been established in collaboration with the Swedish company, HEXAGON which they are using for the handling of 1000 bar pressure of hydrogen. For LH2, land vehicle fuel tanks, ISO 13985: 2006 must be used to design the tanks. For CGH2 and hydrogen blends, for long vehicle fuel tanks, ISO 15869: 2009 can be used.

2.6.2 European Agreement Concerning the International Carriage of Dangerous Goods by Road (ADR)

There are no specific guidelines or limitations by the Norwegian government in the pressure or quantities of gaseous hydrogen transported by roads, provided that the cylinders and the pressure valves comply with the ISO standards and are marked CE. However, the quantities per trip are restricted by truck weight limitations. The UN-Model regulation, ADR, and the European Transportable Pressure Equipment directive (1999/36/EC – "TPED") strictly regulates the transport of CGH2, which (Reg 2008) restrict the increase in payload of hydrogen trailers and the cylinder/tube volumes by 450l/3,000l. ADR includes hydrogen in the list of a dangerous good, Category 1 "Extremely Flammable Gas" H220 or as compressed gas, H280. It falls in class 2, classification code 1F, danger class 23. The tunnel restrictions apply to categories B, C, D, and E when transported in a tank. When transported in tunnels of categories D and E when transported in other than tanks. In Norway, the restrictions of transportation through tunnels apply to subsea tunnels between Ellingsøy and Valderøy near Alesund during the period 0600-2400. At Hvalertunnelen, the transport of hydrogen requires Road traffic central's permission. Annexes A and B in the ADR include hydrogen, and other dangerous goods, or substances whose transportation by road is either prohibited or only authorized under certain conditions. The safety factor is taken to be the ratio between the burst pressure and the nominal operating/fill pressure, which in ADR is taken to be 3 for gas cylinders and tubes with composite materials, referenced for application areas, maximum volumes, and operating pressures.

In Norway, the Norwegian public Roads Authority is responsible for the regulations of ADR driver and vehicle certification. The driver must hold an ADR certificate (section 8.2.1, ADR/RID 2017). Chapter 5 of the ADR Book can be used for establishing the consignment procedures. In section 5.4.1, ADR instructions about handling emergencies and accidents during transport are addressed. Since there is a lack of relevant regulation, HEXAGON, the global technology group headquartered in Sweden has joined hands with Standard Norway for developing ISO standards (ISO 17519) for hydrogen (HexagonComposites, 2015). With the type IV cylinders, Hexagon through its ISO 17519 standards, has been able to use type III cylinders for pressures below 1000 bar.

The CGH2 and LH2 states are considered for the analysis. For the CGH2 states, the truck types are tube trailers. Depending on the safety level required, different tank types as suggested by (Barthelemy, Weber et al. 2017) could be used, with type IV being the more mature type of storage material. Different metals, polymers, or composites could be used in the construction of such storage materials (Barthelemy et al., 2017). Based on the demand volumes, the CGH2 state is more suited to small stations and low demands (Yang and Ogden, 2007)therefore, the most feasible transporting distances for the CGH2 are usually short for example less than 200 miles (320 km) (Yang and Ogden, 2007), Drive 2017, EU 2019). The upper and higher limits for pressures of 200 and 500 bar are in common practice

in the EU and are used for carrying up to 600 and 1100 kg of amounts of hydrogen respectively (EU 2019). The storage pressure vessels with 200 to 300 bar and a trailer can carry up to 6,200 Nm^3 of H2 for trucks subjected to weight upper bound of 40 tons (EU, 2019). For LH2, cryogenic road tankers are used. The materials used involve monolithic metals, polymer, and metallic composites (Mital et al., 2006). In the case of the cryo-compressed mode of delivery, carbon fiber can be used as a tank material (Ahluwalia et al., 2018) and CGH2 be economically distributed within a radius of 600 miles (966 km) (Drive 2017). Table 4 summarizes the discussion for CGH2 trailers.

Table 4: CGH2 transportation specifications

Description	Comments
Truck types	Tube trailers
Storage Vessels	Type I, II, III, and IV (Barthelemy et al., 2017)
Materials Selection	Metals (Aluminium 6061 or 7060, inox or chrome molybdenum steel), polymers, carbon fibers, composites (Barthelemy, Weber et al. 2017)
Suited demand volumes	Suited to small stations and low demands(around 300 kg per truck)(Yang and Ogden, 2007) (Drive, 2017)
Suited Distances	Short ranges (less than 320 km) (Simbeck and Chang, 2002)
Pressure (Normal Practice in Norway)	200 bar (Hylaw 2020)
Pressure (ADR 6.2.5.5 regulations for type IV tanks)	500 (Hylaw, 2020)
Mass (Normal practice in Norway)	600 kg (Europe, 2020) (Baldwin, 2017)
Mass (Upper limit for type IV composites)	1100 kg(Europe, 2020)

Hydrogen safety is a major obstacle for hydrogen to be replaced immediately with fossil fuels. The safety of hydrogen should be considered in-depth throughout the hydrogen value chain, from its production to its usage by the end-user. Bowtie methodology is a common way to illustrate the safety aspects. The critical event is the loss of containment (LOC), which can happen in open or confined spaces. In open spaces, the consequences are likely to be ignition, fast flame propagation, and explosions. For non-confined spaces, the flames can result in an explosion, leading to the release of huge amounts of energy. For enclosures,(Burt, 2015) concluded that the pressure peaking following an non-ignited release of hydrogen is hazardous and therefore this must be properly considered for the indoor usage of hydrogen. Since, realistically, hydrogen would ignite immediately after it is released, the scenario of release from TRPD after ignition(Thermal pressure release device) is more hazardous(Xu and Wen, 2012). For LH2, BLEVE (Boiling Liquid expanding vapor explosion) and RPT (Rapid Phase Transition) are atypical accidents. It has been established that hydrogen damage is the major cause leading to the critical event (Ustolin, Paltrinieri et al. 2020). A failure of containment for LH2 presents a different risk picture. The loss of containment from a liquid storage system may result in pool formation, owing to the high density of the liquified hydrogen as compared to air. The health hazards of hydrogen are cold burns, high-temperature burns, and asphyxiation, and so on (ISO 2004). Safe handling of hydrogen and hydrogen systems can help in the reduction of accidents. This can be significantly improved by providing safety training and promoting effective communications to the team involved in handling hydrogen.

2.7 Design of protective wall for overpressure: types of safety walls

The barrier walls, to reduce the severe consequences of the accidents, might also produce other hazards if the configuration is not well thought of. The other hazards could be in several forms, e.g wrong configuration can cause turbulence within hydrogen jet, which might result in higher overpressures as compared to free jets. The importance of a safety wall can be stressed from the study carried out by (Dadashzadeh et al., 2018), that defines the hazard distance for onboard hydrogen storage tanks for a blast wave to be 1.68 m, and 35 m for fire hazard, whereas for the serious injury distances are 13.4 m and 555 m, respectively. According to ADR section 9.3.3, the driver's compartment shall be separated from the load compartment by a continuous wall.

(Willoughby and Royle, 2011) carried out a detailed study to evaluate the interaction of hydrogen releases with walls and barriers. The study considered NFPA (National Fire Protection Association) codes that suggested the use of a 60-degree inclined wall for effective protection against jet fires as opposed to the vertical, 90-degree walls. However, the study concluded that for effective protection against both the blast overpressure and jet fire, it is safer to use the vertical barrier, as the only disadvantage in such a scenario would be lesser heat flux reflected the leak source.

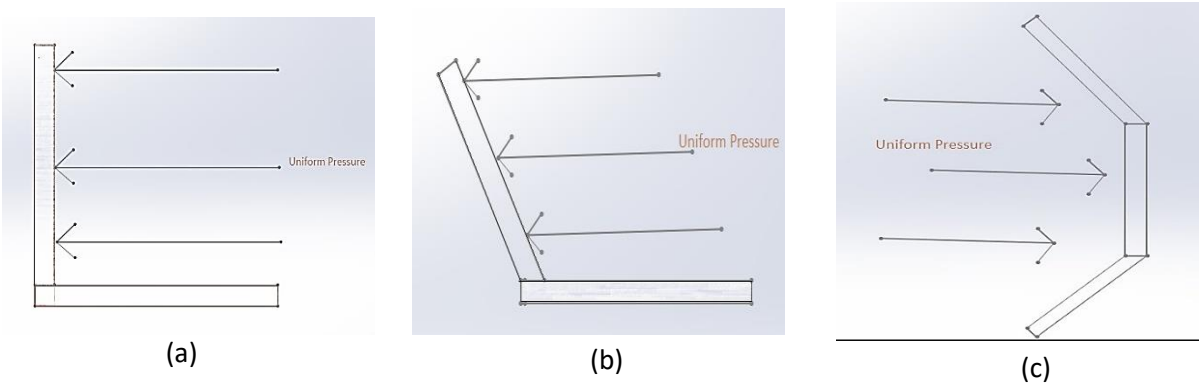

Figure 2: Different Wall orientations against Uniform Pressure (a) Single horizontal (b) Single Inclined wall (c) Three inclined walls configuration

The study is focused on the design options for the blast loading of the sacrificial wall against hydrogen overpressure in case of an explosion. Several design parameters have been considered in the analysis. According to (Gebbeken and Döge, 2010), the overpressure of a blast wave strongly depends on the two key parameters, the stand-off distance and the duration of peak overpressure. The analysis starts with the consideration of protective wall material, and by varying different steel structures, an optimum choice where the safety and the mass of the protective wall have been prioritized. A comparison of variable wall sizes has been made and the effects on the design have been recorded. Since the blast pressure decays very fast, a higher standoff distance between the tank and the sacrificial wall is very useful. (Gebbeken and Döge, 2010) investigated four cross-sections, circular, quadratic with a corner directed to the explosion center, quadratic with an edge directed towards the explosion center, and a rectangular section. The study concluded that the circular section is the most effective choice as the shape showed relatively lower peak overpressure and lower maximum impulse per unit length. The study also concluded favoring of the adoption of nonconvex shapes against the convex shapes, and usage of energy absorbing materials. Figure 3 shows the pentagonal wall between the driver's cabin and the tanks.

Figure 3: Design inspiration for the barrier wall courtesy (Weldship Corporation, 2021)

3. Methods and Tools

3.1 Literature Review

A narrative review approach was adopted to provide the foundation data for this study. This type of approach was useful for gathering a volume of literature for critical and objective analysis of state of the art on hydrogen technologies. In the literature, ORIA and ScienceDirect databases were used as research databases. The main keywords used in the literature review are listed as follows.

- Compressed gaseous hydrogen
- Safety barriers
- Hydrogen safety
- Hydrogen tank
- Hydrogen risk assessment

3.2 Risk Assessment Process

As the loss of containment via transport of hydrogen can have severe consequences, a detailed risk assessment must be employed, the schematic of which is shown in Figure 4. The first step is to thoroughly investigate the probable key consequences, which is followed by the hazards identified through the techniques like PHA (preliminary hazard assessment), or HARA (hazards and risk assessment). This can be also be carried out by using either HAZOP (Hazards and operability study) or FMECA (Failure, modes, and effects criticality analysis) which are widely accepted methods of identifying risk sources (Kikukawa et al., 2009). Since the current study is focused on the driver's cabin safety, thus the blast wave and fireball are identified as key consequences, as these follow catastrophic rupture in a fire, and thus have much higher safety distances as compared to jet fire (Dadashzadeh et al., 2018). While the results of modeling can indicate the fatalities, serious and minor injuries, the frequency analysis would give the tank rupture frequency which gives the foundation for evaluating risk. The evaluated risk is then checked against the tolerable risk, and further risk reduction measures are introduced in case the evaluated risk is greater than the tolerable risk. The results of the overall process results in obtaining overall safety requirements of the system.

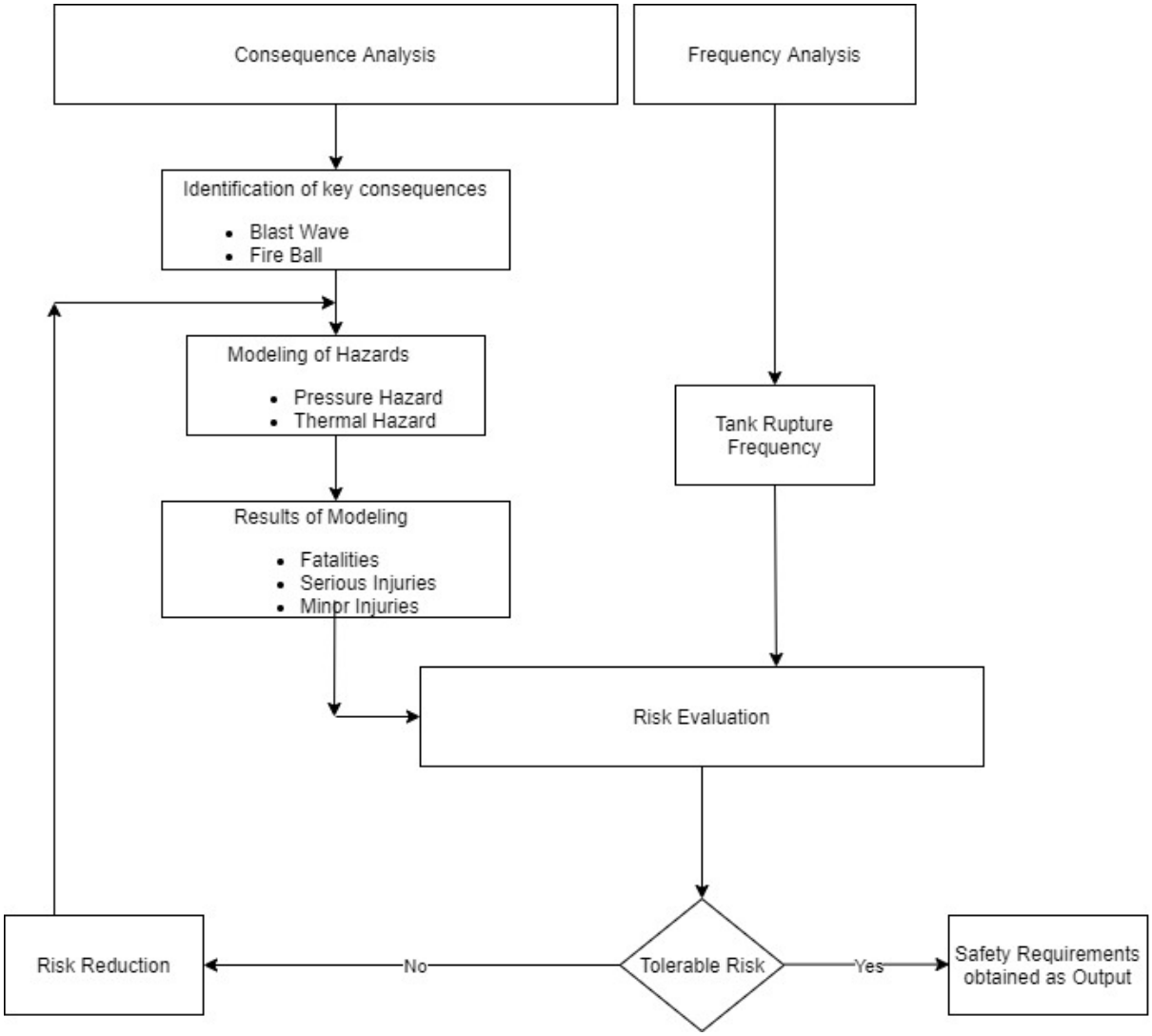

Figure: 4 Risk Assessment Process

3.2.1 Bow-tie

Bow-tie methodology is a well-known methodology for illustrating the safety aspects of a critical event. The left-hand side of the bow-tie indicates threats and the subsequent preventive barriers whereas the right-hand side represents the critical event and their reducing measures as depicted in Figure 5. In this study, the focus is on the right-hand side, in particular on the design of a safety wall to reduce harmful consequences from the catastrophic rupture of the CGH2 tank as a critical event.

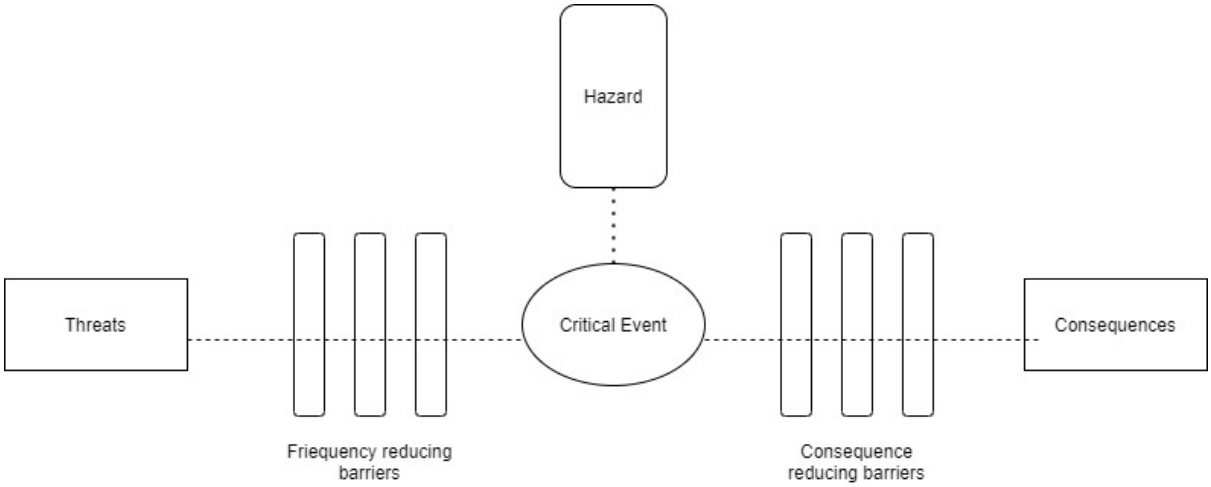

Figure 5: Bow-tie methodology for visualizing risk elements leading to consequences (Risk, 2020)

3.2.2 Tank Rupture Hazards Analysis

The calculation of risk implies the assessment of two main hazards from a tank rupture, blast wave and fireball (Molkov et al., 2019). The study is focused on the catastrophic explosion, due to the loss of containment of hydrogen. Therefore, the study addresses the right-hand side of the bow-tie diagram, which involves the design of consequence-reducing hazards. The objectives of the case study are as follows.

a) the design of the safety wall should be able to deflect jet flame and protect the cabin from other solid objects in case of a hazardous event.
b) the wall should protect from the overpressure

In this study, the knowledge of the unintended release of hydrogen is important to design an effective safeguarding barrier. In the case where hydrogen is released but remains non-ignited, the knowledge related to hydrogen flammability envelope and the concentration field is important to determine the consequences and ensure safety under such loss of containment issues (Houf et al., 2009). In the other case where a high pressure of hydrogen is ignited, a turbulent jet is formed. In that case, the details regarding the length of flame, and heat flux distribution is important for safety. Such a scenario can be catastrophic, depending on the effective leak diameter, source tank pressure, and the free jet flames can be quite extensive in length and radiation, thereby becoming quite capable of resulting in consequences that might involve accidents.

3.3 Software Overview

In this study, SolidWorks 2020 Student Edition has been used to carry out the finite element analysis (FEA) for the scenario of modeling the barrier wall against the effects of high pressure and thermal loads. FEA is a powerful engineering tool widely used by design engineers during the product development phase to analyze the design of the product. SolidWorks Simulation is a commercial implementation of FEA capable of solving common design-related problems, such as displacement analysis, the strength of materials analysis, and heat flow (Kurowski, 2013). The first step was to design the chassis of the truck and the protective wall. During the part design, the material properties are defined. After the assembly, the model geometry is discretized in finite elements, much smaller than the overall model itself. and the mesh is effectively built-in SolidWorks Simulation. According to

(Kurowski, 2013), there are essentially three steps in the FEA modeling with SolidWorks, which were followed in the study.

1. Pre-processing the FEA model, involving model definition and splitting into finite elements, or mesh.
2. Solving, to get the results.
3. Postprocessing to analyze the results

The study could be subject to several unavoidable errors as the formulation of a mathematical model introduces numerical errors. (Kurowski, 2013). These errors can be significantly reduced by building the right mathematical model (accurately defining loads, restraints, material properties, and selecting the most appropriate type of analysis, e.g., linear static), carefully considering and choosing the right number of mesh elements, and finally, properly interpreting the results. While there were plenty of other softwares to carry out the finite element analysis (e.g., ProEngineer, CATIA and ANSYS, etc.), SolidWorks is the preferred option as it has a simpler interface, has accurate results when the problems are setup correctly, and the results generally fall within 1 percent of industry benchmarks (SolidWorks, 2021). Also, NTNU has the license for its student version which was also a key factor in the selection of SolidWorks as the software.

3.4 Methodology Steps for the Finite Element Analysis

Once the important relevant formation about the materials choice, chassis dimensions, welding and boding specifications, design of barrier wall, design factor of safety, and the external pressure and thermal loads are clear, the FEA can be initiated. The following steps are followed.

1. Design of the assembly, by choosing the initial material for the wall, analyzing the mesh, and refining mesh in the critical regions. Then analyzing the results for the behavior of the safety wall under stress loading.
2. Varying the materials, and choosing the best material based on the strength and mass of the safety wall's material. Generally, a high strength, with low weight and cost is a favorable material for most instances.
3. Analyzing the results to see if the SolidWorks design constraints have been met.
4. Based on the material selected, varying safety wall thickness to see design alternatives.
5. Varying the shape of the safety wall by keeping other parameters constant, give the stakeholder multiple safe design options for choosing the design that suits them best.
6. Suggesting safe design and other consequences reducing barriers.

3.5 Model configurations

The geometry of the model consists of essentially three solid bodies, designed in the part module of SolidWorks, and are then assembled in the assembly module of SolidWorks for the FEA. This model in the assembly is composed of the fixed rectangular orientation, 6307mm X 2400mm, and thickness of 30mm. These dimensions are chosen as per MCE's specifications for the tank given in appendix A.1. The 30 mm AISI steel cold rolled chassis bed thickness remains uniform throughout the analysis and is, therefore, a safe assumption as the stresses are applied parallel to the surfaces. The chassis cannot move because it is constrained with "fixed geometry", thus its thickness is irrelevant. The wall thickness and orientation change are important to optimize the design for safety. Some support structures are introduced to make the design the safest. Figure 7 shows the isometric views of the model used. Figure 6 (a) is the snapshot from the SolidWorks part module showing the chassis bed of 30 mm thickness, figure 6 (b) is also the snapshot showing the safety wall used throughout the analysis whereas figure 6 (c) is the snapshot from the assembly module of SolidWorks where the two parts are assembled. From figure 6 (c), it can be seen that the safety wall has been placed at some distance far

off the end of the chassis. This is done to accommodate the support for the safety wall and keep some safety distance so the deformation at the top does not become an additional hazard for the driver's cabin.

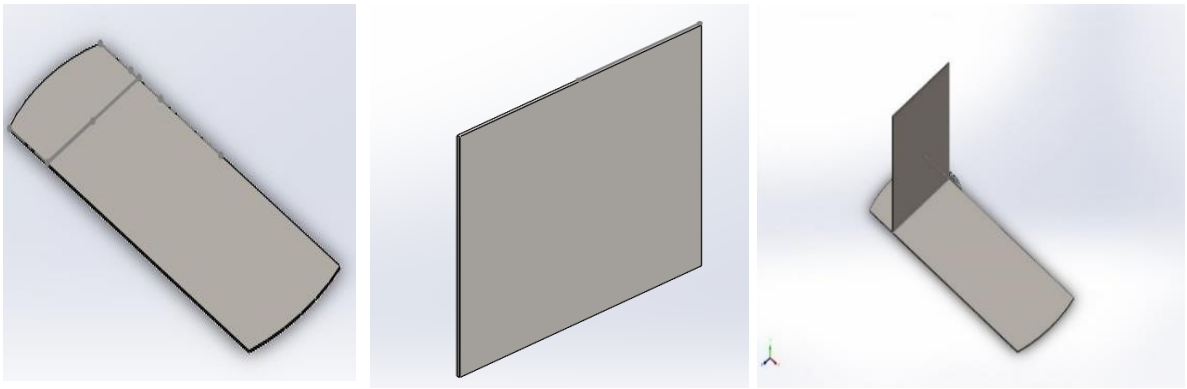

(a) (b) (c)

Figure 6: Isometric views of (a) Chassis bed (b) Simple barrier wall (c) Model configuration for the simplified wall case

In the analysis, initially simple barrier wall without any supports has been used as shown in the figure 6 (a). The material selected based on the simulation results is then used in the model with triangular supports. Initially two triangular supports have been used, which is shown in figure 7 (a). Then the barrier is further reinforced with the third triangular support. The last model configuration considered is pentagonal wall with and without supports. This has been shown in the figure 7 (b).

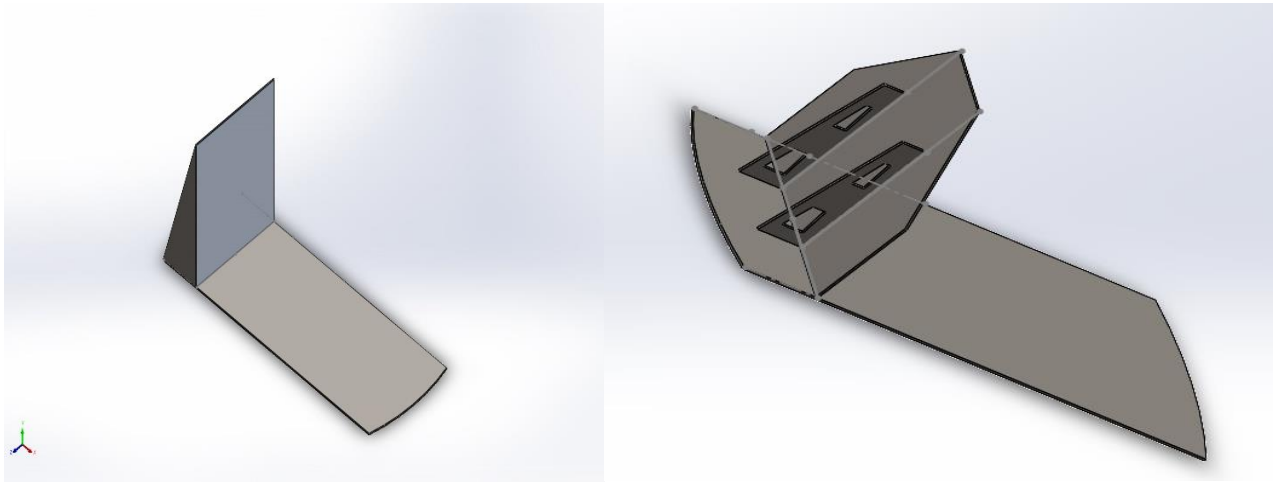

(a) (b)

Figure 7: Design of barrier wall a) with reinforced triangular supports (b) Pentagonal wall with supports

Table 5 lists the dimensions used for the chassis wall and the safety wall. While the FEA starts by analyzing material with the same 30 mm thickness, the width is varied in the analysis to find the optimum design. The rest of the factors remain constant throughout the FEA. Table 5 also shows the mass of the pentagonal wall.

Table 5: Design specifications for chassis bed and different types of safety wall

Dimensions of Chassis bed and Safety Wall	
Width of chassis bed	2400 mm
Length of chassis bed	6307 mm
The thickness of the chassis bed	30 mm
Height of Safety wall	2584 mm
Mass of chassis bed	3584 kg
Mass of 30mm simple wall (AISI 1020 cold rolled steel)	1464 kg
Mass of 30mm pentagonal wall (AISI 1020 cold rolled steel)	1233 kg
Mass of 50mm pentagonal wall (AISI 1020 cold rolled steel)	2245 kg

Mesh specifications and boundary conditions

Throughout the analysis, high-quality mesh has been used. In the analysis, the total number of elements in the mesh on average was above 25,000, whereas the total nodes were above 40,000. The percentage of elements with an aspect ratio greater than 10 was only 1.15. The minimum element size for the mesh was about 5 mm. In the area of the welding between the base and the wall, finer mesh elements were used as that area was more critical to the analysis. Figure 8 (a) shows the course mesh that is generated with default SolidWorks mesh settings. By refining the mesh, much finer mesh particles have been obtained, as shown in figure 8 (b).Several important constraints are used in this study. This is important to have the specific stresses simulated in the critical areas of failure. For the component contacts, the assembly feature of weld has been used. The connect type between the bed and the wall has been chosen to be welds/adhesives. It is assumed that the adhesive is thin, therefore not allowing the shear (rigid adhesive). For the fixture's constraint, a fixed fixture under the chassis bed has been modeled. Uniform pressure of 400 kPa on the face of the wall has been applied. No vehicle damping, vibration has been considered. Also, no thermal stresses and radiation parameters have been applied to keep the analysis restricted to only high-pressure analysis. Figure 8 (c) shows the constraints used in the simulation. The direction of the application of uniform pressure on the boundary, fixed geometry and weldment constraint are shown.

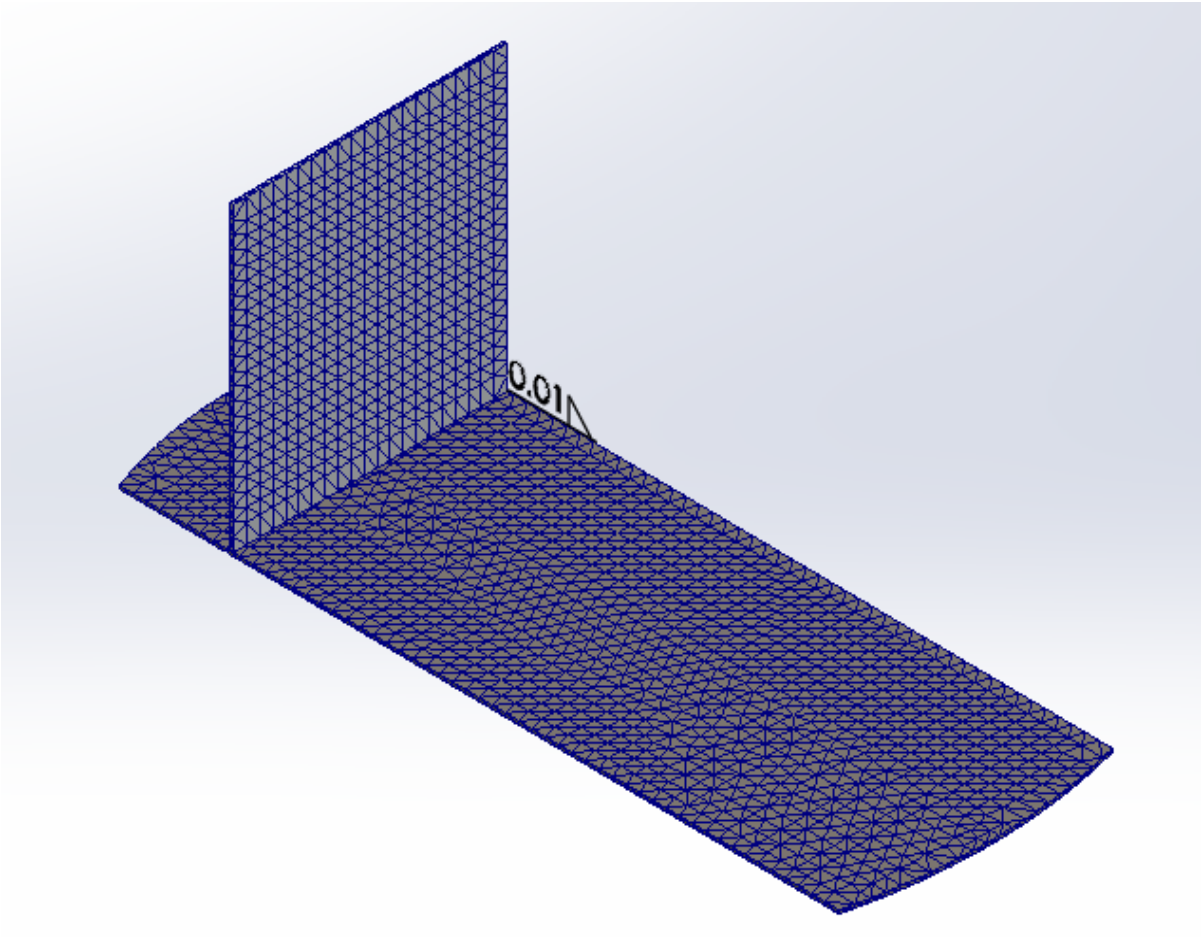

(a)

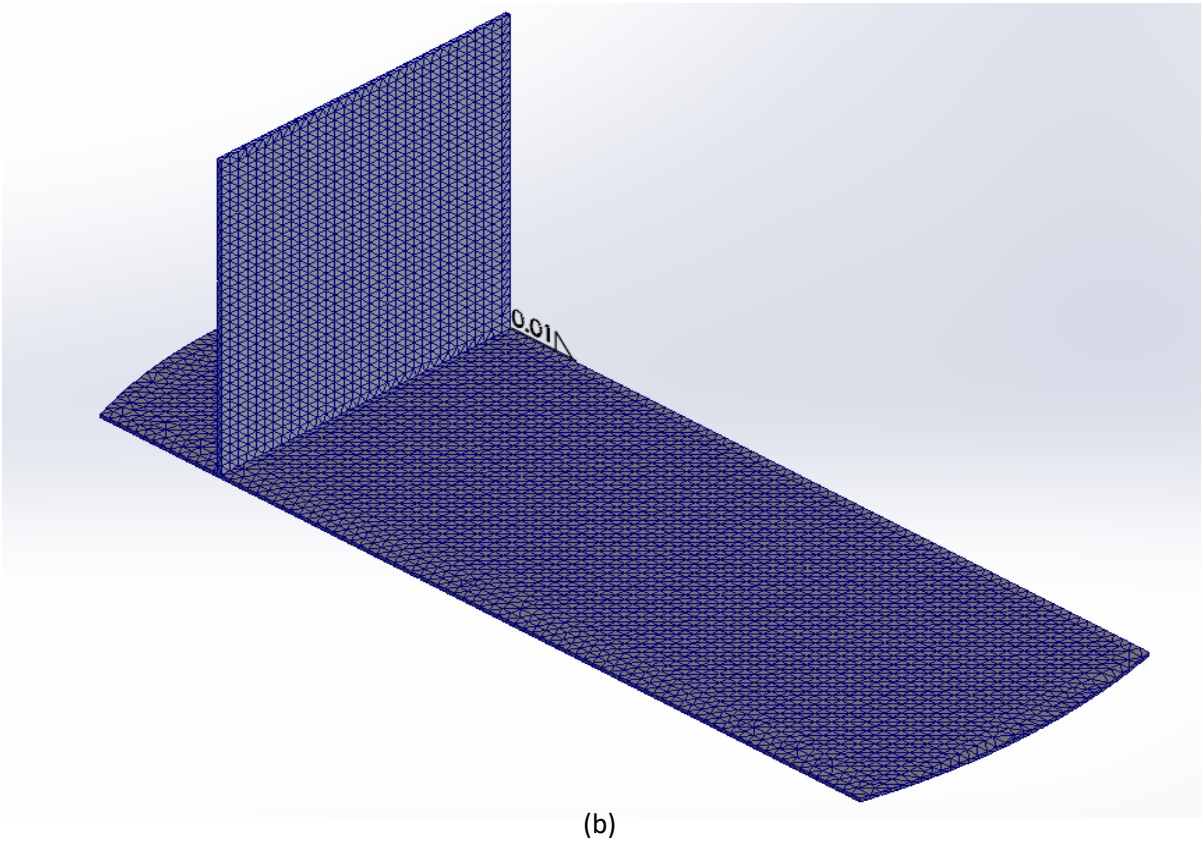

(b)

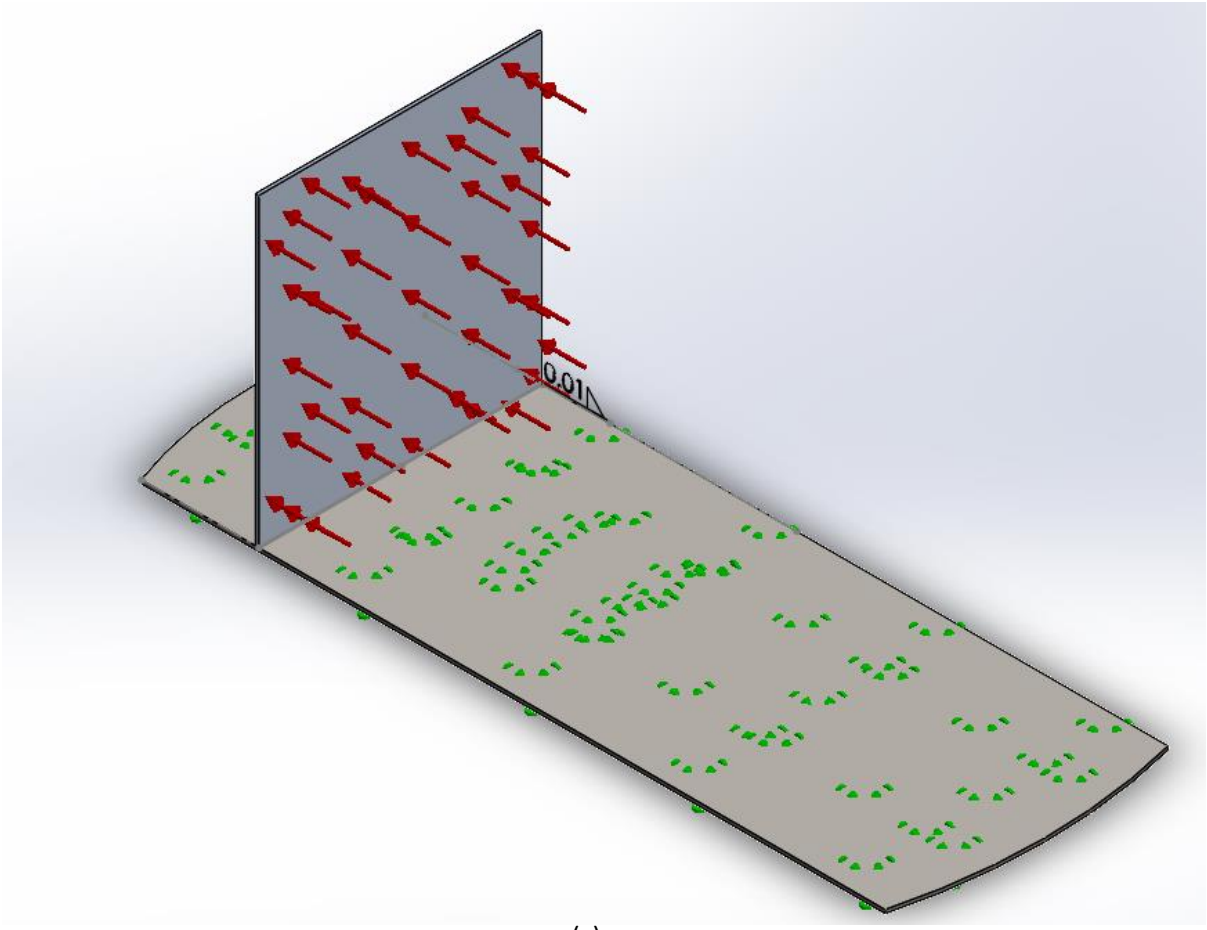

(c)

Figure 8: Mesh and boundary conditions description (a) coarse mesh (b) refined mesh (c) model with fixed geometry, pressure and weld constraints

4. Results

The narrative review of the literature has resulted in providing the foundation data for the Finite element and modeling and analysis. The literature review provided a solid foundation regarding hydrogen properties, hydrogen safety issues during production, storage, and transportation. According to (Zhiyong et al., 2010), the physical explosion produces the longest harm effect distances for instantaneous hydrogen release, whereas the worst case of confined vapor cloud for continuous release produces the most severe results. Overpressures created via hydrogen combustion can vary based on the scenario, and the least significant is flash fire, as hydrogen is consumed rapidly (LaChance et al., 2011). In most cases, deflagration occurs when the flame speed is subsonic (Zhiyong et al., 2010). (Molkov and Kashkarov, 2015) addressed the knowledge gaps in hydrogen safety for predicting the deterministic separation distance defined by the parameters of the hydrogen blast wave caused by a high-pressure hydrogen tank rupture, with consequent ignition of its content. The study of such a catastrophic event caused by a 72.4 L, 34.3 MPa storage tank resulted in an overpressure of 300 KPa at a distance of approximately 2m from the tank. According to the study carried out by (Kashkarov et al., 2020), the intensity of overpressure can depend on several factors like storage volume and pressure. (Bang et al., 2017) used FLACS for hydrogen containment in the range from 10 to 400 kg under open-air conditions. It was concluded that the overpressures increased with greater fuel mass, and for the 400 kg explosion, overpressure was approximately 75 kPa. Given that we maintain at least a 2 m distance between the tank and the safety wall, the idea is to design a wall that should withstand the conservative 400 kPa pressure. For simplicity, the pressure is taken as uniform pressure.

To select the right material among several options, it is important to consider both physical (e.g density, melting point, etc.) and mechanical (strength, ductility, etc.) properties. According to (Ashby and Johnson, 2013), there are four different ways to select the material which are:

1. Deductive reasoning (selection by analysis)
2. Inductive reasoning (selection by reasoning)
3. Selection by similarity
4. Selection by inspiration

In this study, the most suited approach is to use deductive reasoning, where the selection of material is based on using analytical tools (e.g SolidWorks in the current case), which is also the traditional engineering approach to materials selection (Ashby and Johnson, 2013). Based on the fact that the company is specializing in steel structures (MCE, 2021), this traditional method of the choice of materials based on informed guessed solutions is focused on choosing the most favorable material steel-based alloy. Therefore, the first step is to limit the analysis to the high-strength steel structures, and then choose the best material as per requirements through the SolidWorks analysis. In the analysis, AISI 1020 cold rolled steel, AISIS 1010 hot rolled steel, plain carbon steel, AISI 4340 Normalized steel, and 1345 Aluminum Alloy have been considered. The last one (Aluminum alloy) is considered for comparison's sake. The material properties have been shown in appendix A.2.

4.1 Design of simple barrier wall to prevent the driver's cabin from pressure shocks.

Initially, the design of the wall has been kept simple without any supporting structures behind the wall to protect the overpressure. In the following subsections, the objective is to specify the most optimum material under the available options listed, and then choose the optimum thickness of the safety barrier wall without any mechanical supports behind the wall.

4.1.1 Choice of Material for the fixed 30mm barrier wall's thickness

In section 4.1.1, the results of the overpressure of 400 kPa on AISI 1020 cold-rolled steel have been modeled. The model shows high stresses near the base of the safety wall as indicated by figure 9 (a). Figure 9 (b) shows high displacements on the top regions whereas figure 9 (c) shows the critical areas for equivalent mean strain (ESTRN) that are in the base of the safety wall. The direction of pressure and the constraint for supporting the chassis bed have been indicated with arrows and dots respectively. For clarity, these are hidden in all the results following figure 9.

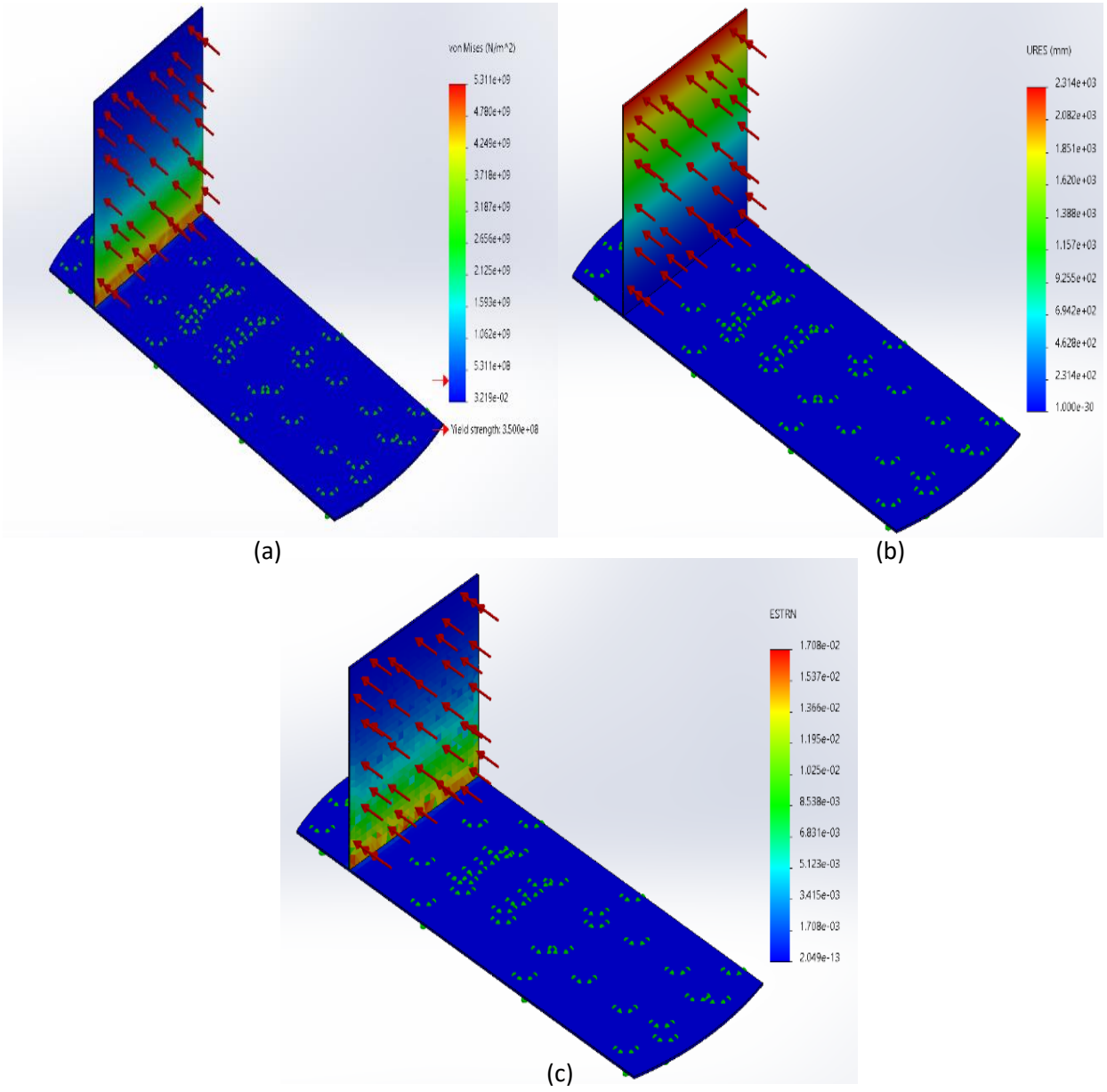

Figure 9: Results for 30 mm wall with AISI 1020 cold rolled steel (a) Von Mises stress (b) displacement (c) ESTRN strain

4.1.1.2 Grid Independence study

Grid independence study is useful for having confidence in the study results. The study was carried out by starting from the default medium-mesh size by SolidWorks for the model. The mesh size was then further reduced to the minimum cell size and the simulation study for coarser, medium, and the finer mesh was carried out. Table 6 compares the results obtained and the error percentages for the Von Mises stress, displacement, and strain. Figure 10 shows the results of the simulation study obtained with the finest mesh size. The material response remains approximately the same, and the mesh size has not significantly affected the results.

Table 6: Grid Independence study

Mesh Type	Number of Elements	Von Mises stress (N/m^2)	Displacement (m)	Strain ESTRN Strain	Von Mises stress Error (%)	Displacement Error (%)	ESTRN Strain Error (%)
Coarser	10615	4.845 E 09	2.146	1.683 E -02	–	–	–
Medium	24327	5.331 E 09	2.314	1.408 E -02	10.031	7.828	27.5
Fine	41882	5.588 E 09	2.327	1.245 E -02	4.821	0.005	13.092

From table 6 it can be seen that the refinement of the mesh reduces the relative error, and the results converge for all three parameters in the analysis. Also, according to Richardson extrapolation (Roache, 1993), the refinement ratio between the two mesh types should be greater than 1.3. We see that the refinement ratio for the medium and coarser mesh is 2.29, whereas the same ratio between the fine and medium is 1.72. Since the refinement ratios are well in the acceptable range, and the relative errors converge with the mesh refinement, therefore the analysis forms the basis to generalize the fact that the study is independent from the grid size. In the rest of the analysis, medium size mesh which has elements of the approximate range of 25000 has been used.

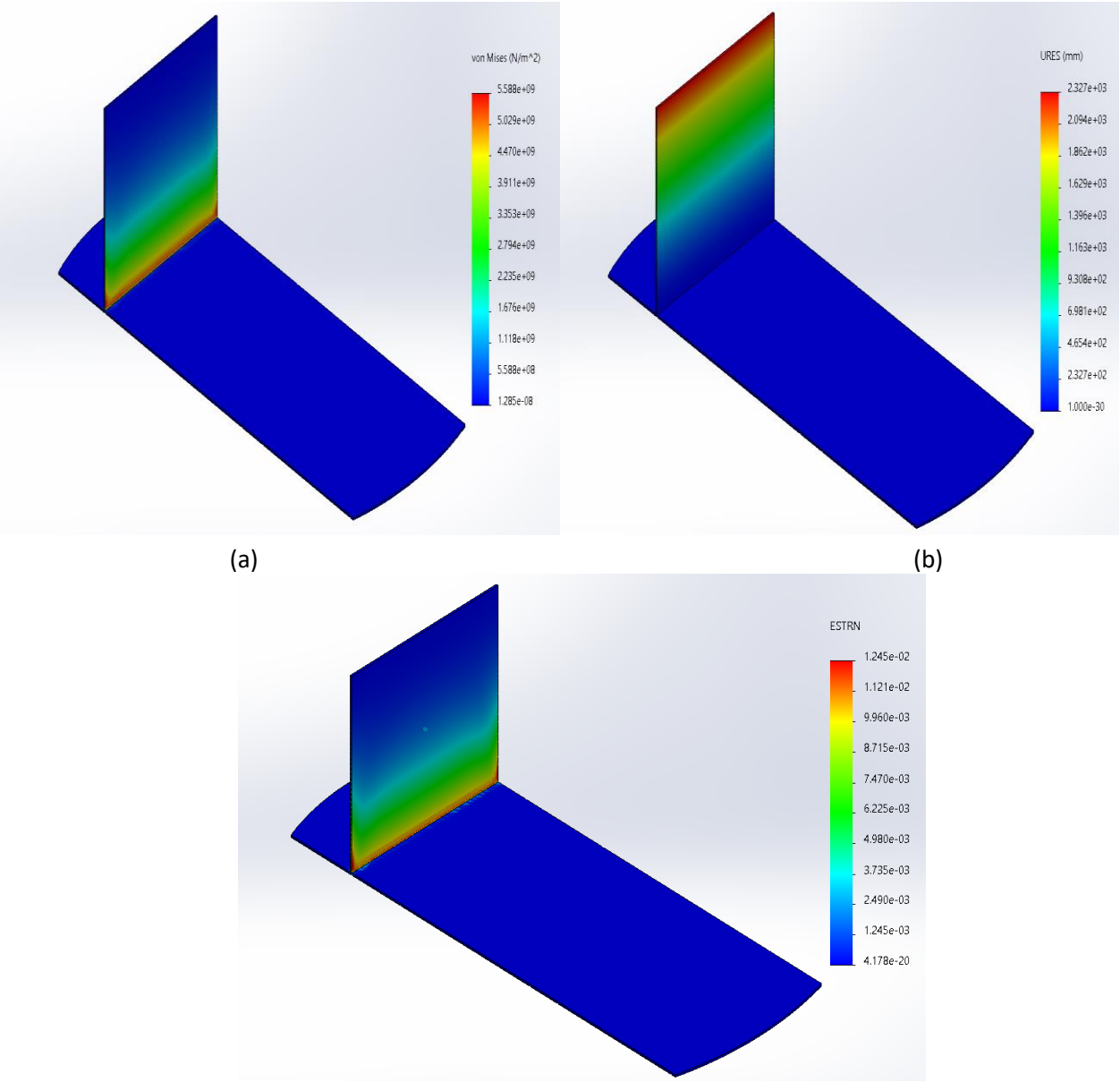

Figure 10: Results for 30 mm wall with AISI 1020 cold rolled steel (a) Von Mises stress (b) displacement (c) ESTRN strain (finest mesh)

In the study carried out in figure 11, the effect of AISI hot rolled steel under the same model configuration has been analyzed. Here the wall shows a better response to the one shown by AISI 1020 cold-rolled steel. However, the material shows more deformation at the top. The barrier wall is

also performing better than the previous one by showing better strain (ESTRN) values. The overall response in terms of weaker areas shown by the stress, displacement, and strain plots remain similar.

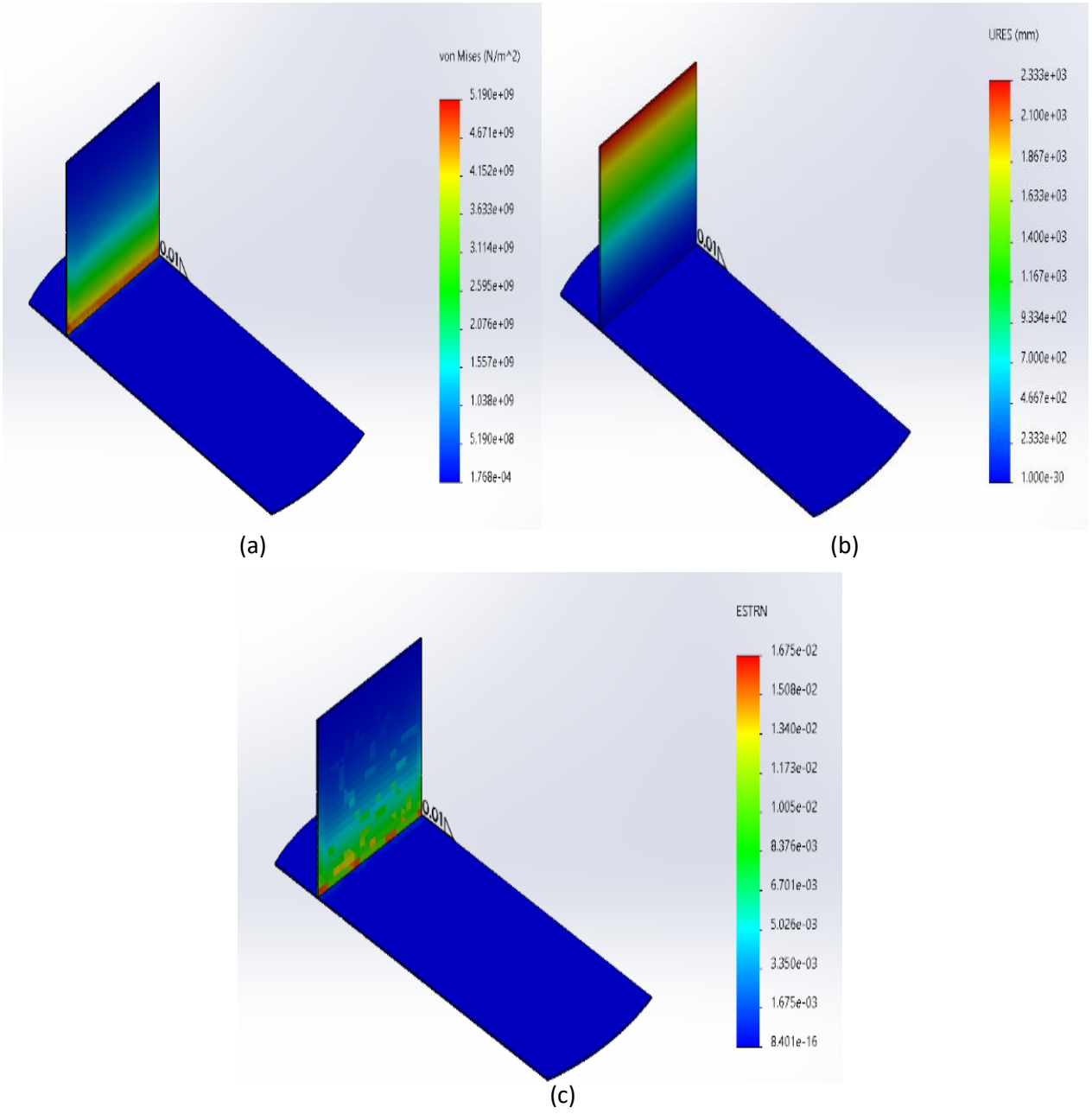

Figure 11: Results for 30 mm wall with AISI 1020 hot rolled steel (a) Von Mises stress (b) displacement (c) ESTRN strain

In the study carried out as shown in the figure 12, effect of AISI 4340 Normalized steel under same model configuration has been analyzed. The stress with this material is lesser as compared to the previously analyzed material AISI 1010 hot rolled steel. Slightly better displacement and strain values can also be seen in figure 12. The overall material response remains similar to the previously used materials.

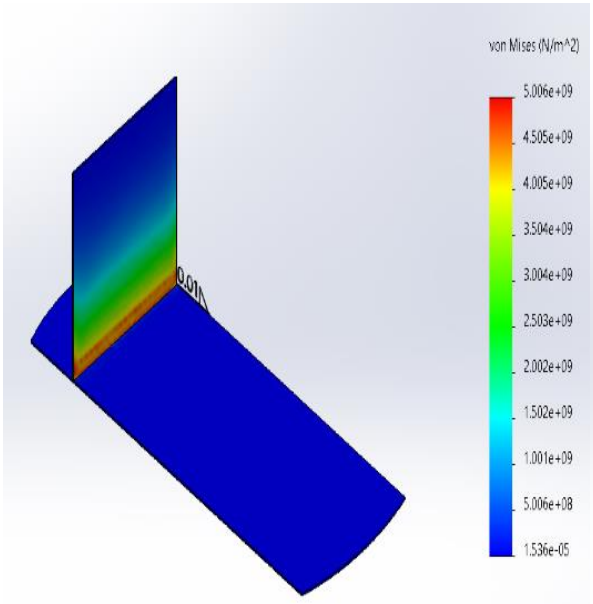

(a)

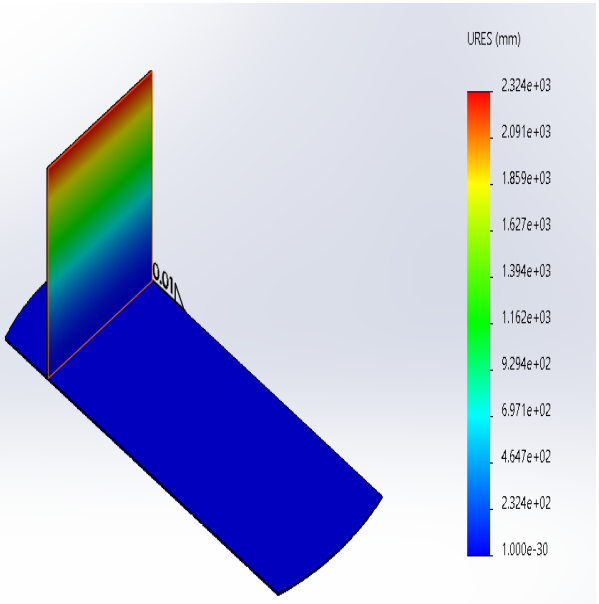

(b)

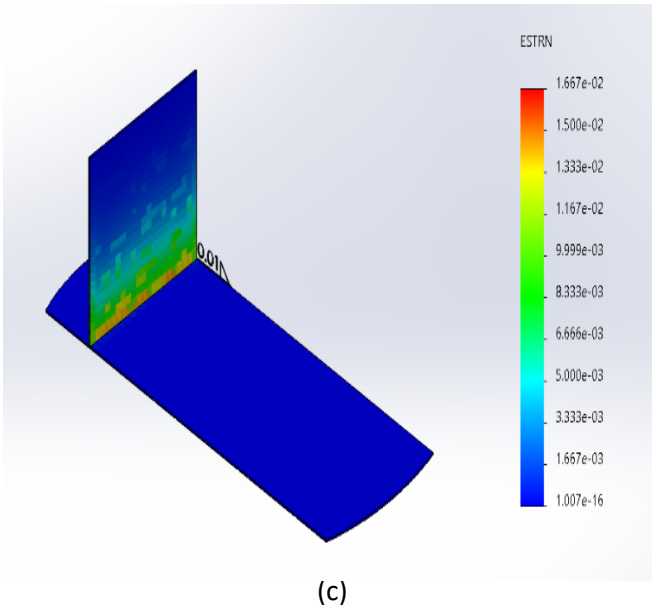

(c)

Figure 12: Results for 30mm wall with AISI 4340 Normalized steel (a) Von Mises stress (b) displacement (c) ESTRN strain

In the analysis carried out in SolidWorks and presented in figure 13, the effect of AISI 4340 Plain carbon steel under the same model configuration has been analyzed. Here, slightly deteriorated behavior to the stress as compared to the previously analyzed AISI 4340 Normalized steel can be seen. However, the maximum displacement for the plain carbon steel is lesser, and the improvement in the strain behavior as compared to the AISI 4340 Normalized steel is also evident.

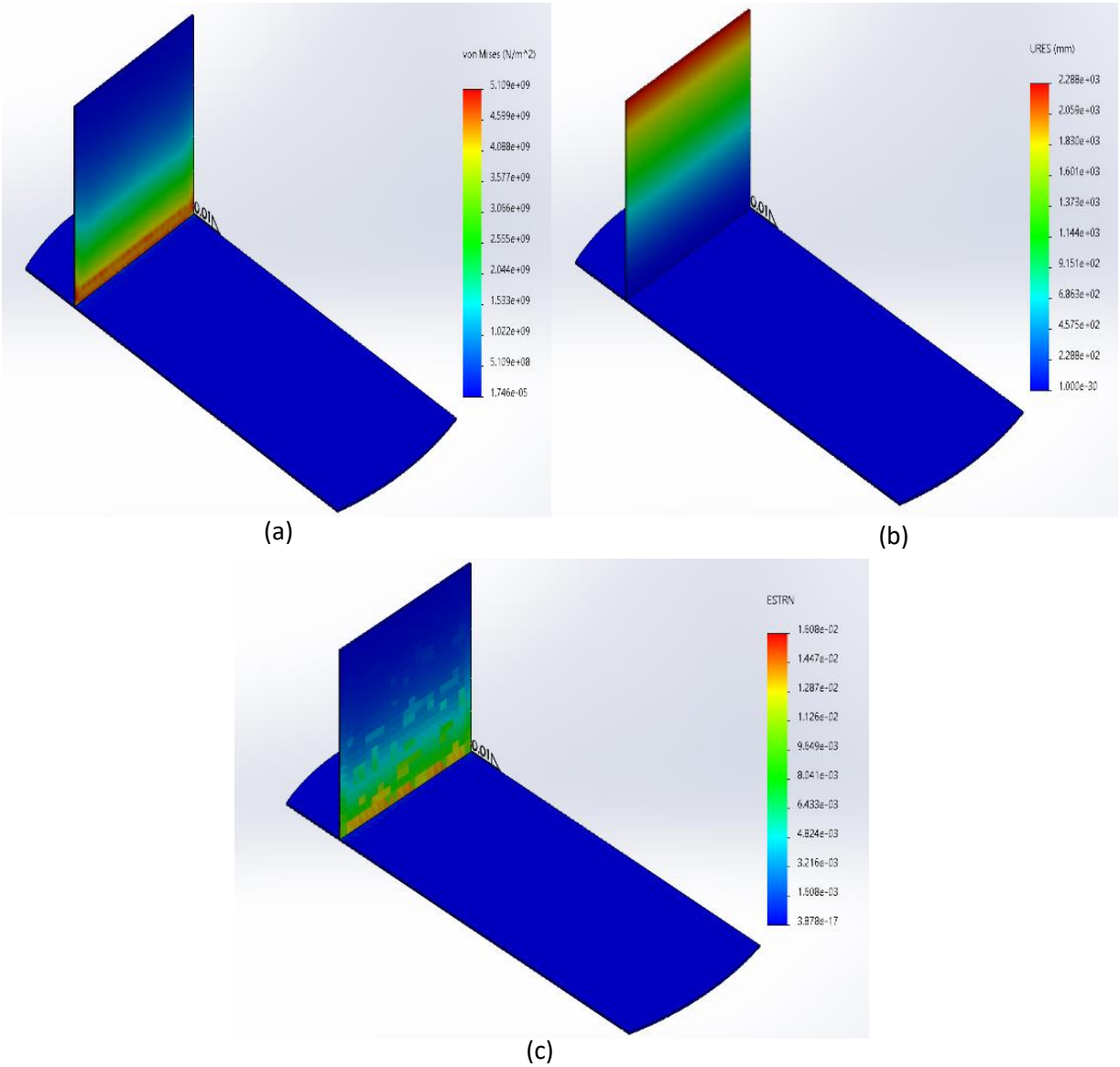

Figure 13: Results for 30mm wall with AISI 4340 Plain carbon steel a) Von Mises stress b) displacement c) ESTRN strain

In the analysis presented in figure 14, the effect of Aluminum 1345 steel under the same model configuration has been analyzed. That is the only non-steel structure analyzed in the study. The material selected has reduced the mass of the wall from 1451 to 500 Kg. Even though the stress value is lesser than the steel alloys used previously in the study, the yield strength is quite lesser than all the alloys. Additionally, the displacement and strain values are quite higher as compared to the steel alloys used in the study.

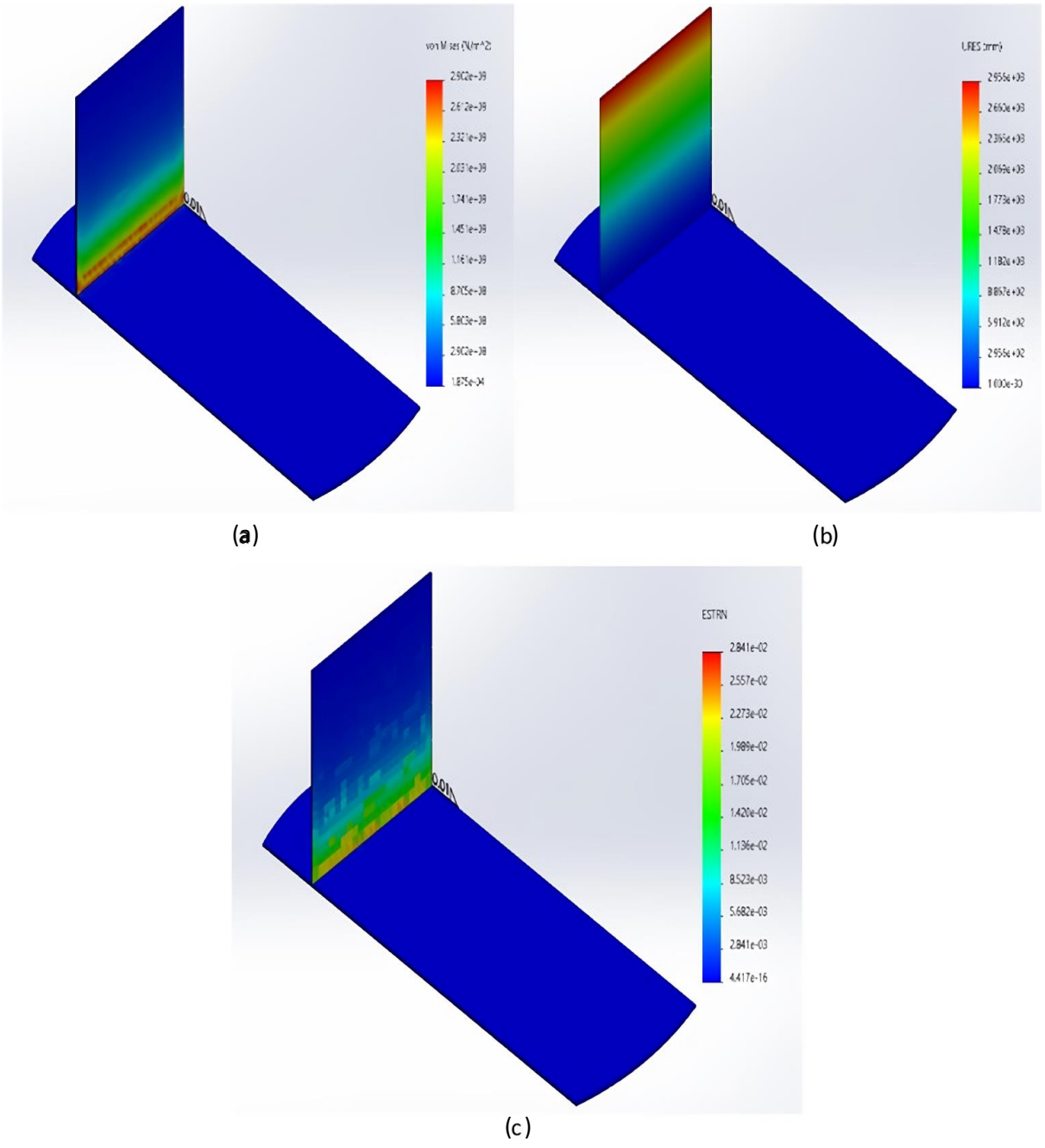

Figure 14: Results for 30mm wall with Aluminum 1345 steel (a) Von Mises stress (b) displacement (c) ESTRN strain

Table 7: Effect of material change on the design

Bed (30mm) (mass = 3,713 kg)	**Wall (30mm)**	**Yield Strength of the wall**	**Mass of the wall (kg)**	**Maximum stress (N/m^2)**	**Maximum displacement (m)**	**Strain (ESTRN)**
AISI 1020 Steel, Cold Rolled	AISI 1020 Steel, Cold Rolled	3.50 E 08	1,464	5.311 E09	2.314	1.708 E-2
AISI 1020 Steel, Cold Rolled	AISI 1010 Steel, Hot rolled bar	1.81 E 08	1,464	5.190 E09	2.333	1.675 E-2
AISI 1020 Steel, Cold Rolled	AISI 4340 Normalized steel	1.80 E 08	1,464	5.006 E 09	2.324	1.667 E-2
AISI 1020 Steel, Cold Rolled	Plain Carbon Steel	2.21 E 08	1,451	5.109 E09	2.283	1.608 E-2
AISI 1020 Steel, Cold Rolled	1345 Aluminum Alloy	2.76 E 07	500	2.902 E 09	2.956	2.841 E-2

In table 7, the results overview of the first set of simulations is provided. It is clear that the yield strength of the material is lower than the maximum stresses in the areas as is illustrated by the stress diagrams. The maximum displacements are also reasonably high and therefore a more detailed analysis should be carried out by considering other parameters. However, it can be seen that the AISI 1020 cold rolled steel and plain carbon steel in the analysis offer comparatively better results, due to higher yield strengths, lesser maximum displacements at the top, and lighter mass. Therefore, AISI 1020 cold rolled steel is chosen as a material for the wall in the further analysis as this industrial material has high strength, ductility, and good weldability (Kelly et al., 2019)

4.1.2 Effect of the thickness of the barrier wall

Now the effects of the safety wall's thickness must be observed. SolidWorks simulations have been carried out by varying wall thickness from 20 mm to 70 mm. The same constant pressure of 400 kPa has been applied directly on the safety barrier wall and the results are noted for the wall thicknesses of 20, 30, 50, and 70 mm. The material for the safety wall is the same AISI 1020 cold-rolled steel. The corresponding mass of the safety barrier walls and the material response to the stress in the form of stress, displacement, and strain have been noted for each of the four scenarios.

For the 20 mm wall, the effects of overpressure have been modeled as shown in figure 15. Extremely high values of stress can be observed in the base of the wall where it is welded to the chassis bed. High deformations on the top and high strain values can also be seen in the figure.

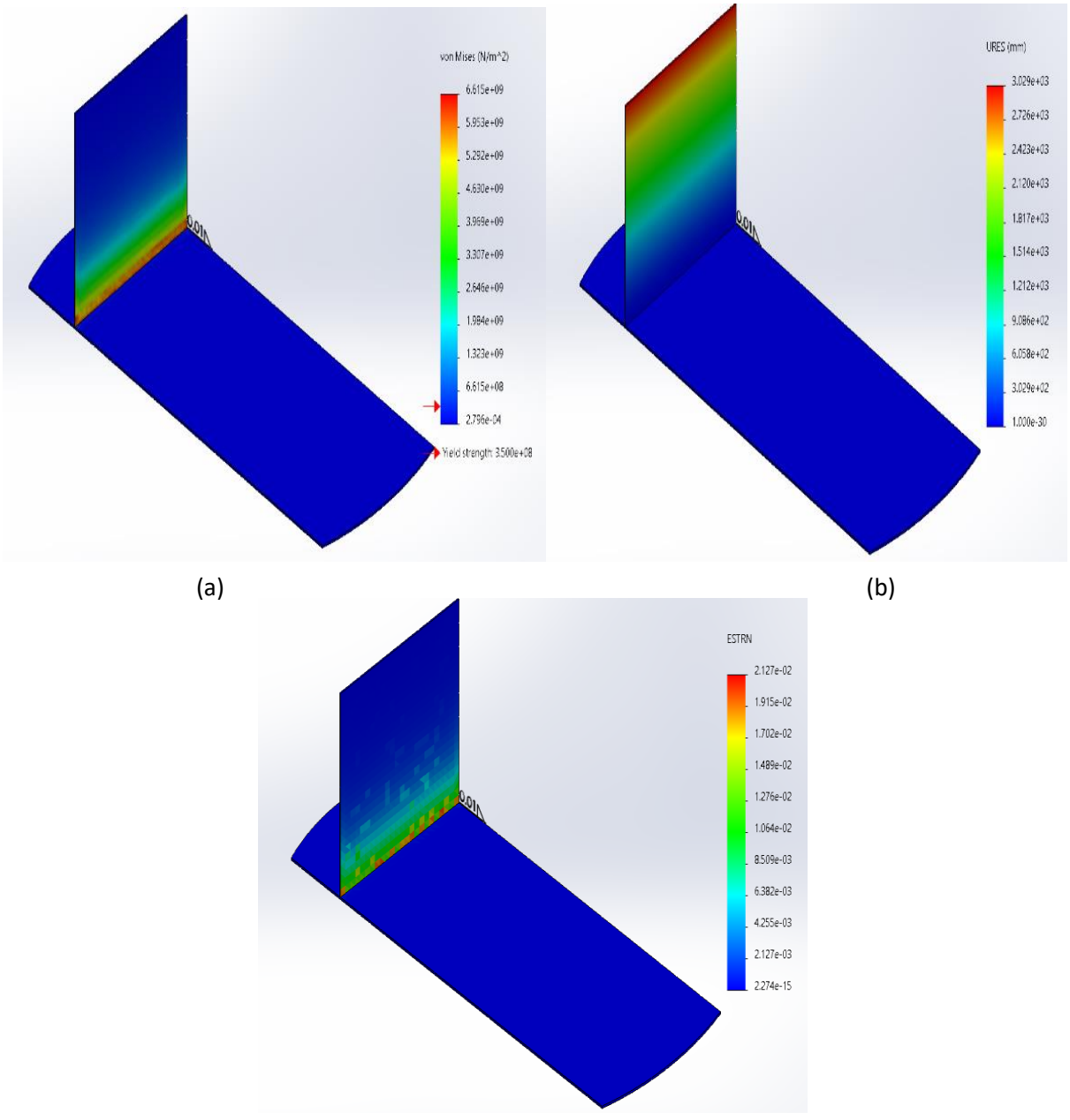

(a) (b)

(c)

Figure 15: Results for 20mm wall AISI 1020 cold rolled steel (a) Von Mises stress (b) displacement (c) ESTRN strain

By increasing the thickness of the wall to 30mm, the effects can be seen in figure 16 which are noted in table 8. For the 50 mm thickness of the safety barrier, the analysis carried out in SolidWorks is shown in figure 16. The effect of the increased thickness is evident, as the material becomes safer with the increased thickness. Stress, displacement, and strain values are significantly reduced.

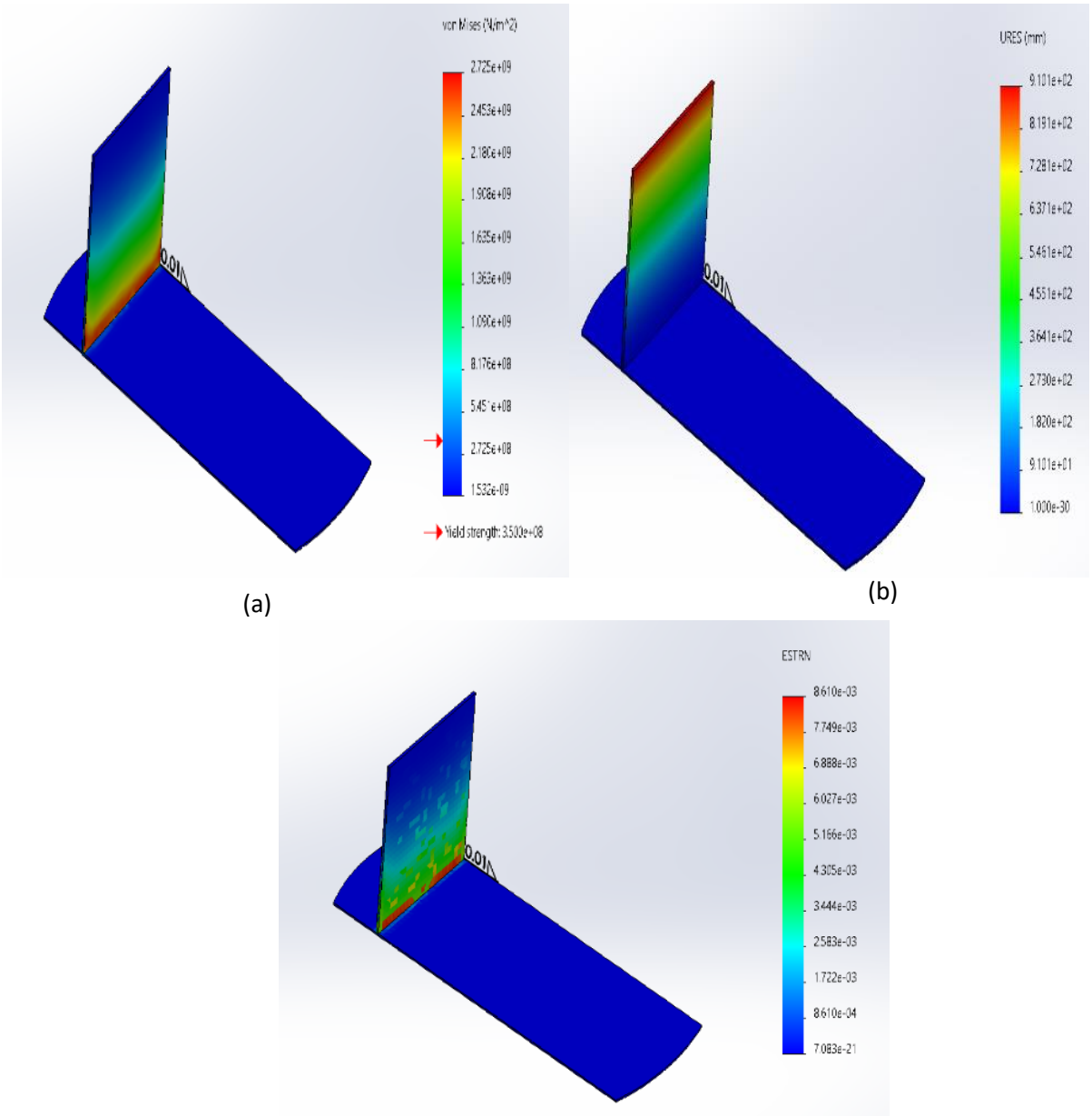

Figure 16: Results for 50mm wall AISI 1020 cold rolled steel (a) Von Mises stress (b) displacement (c) ESTRN strain

For the 70 mm thickness of the safety barrier, the analysis carried out is shown in figure 17. With 70 mm wall thickness, the displacement has been reduced to 0.359 m, whereas the strain value has been reduced to approximately 4.8 E-3, however, the improvement in the stress behavior is still not good enough to rely on the heavy wall of 3416 Kg. Following are the results under the same model configuration.

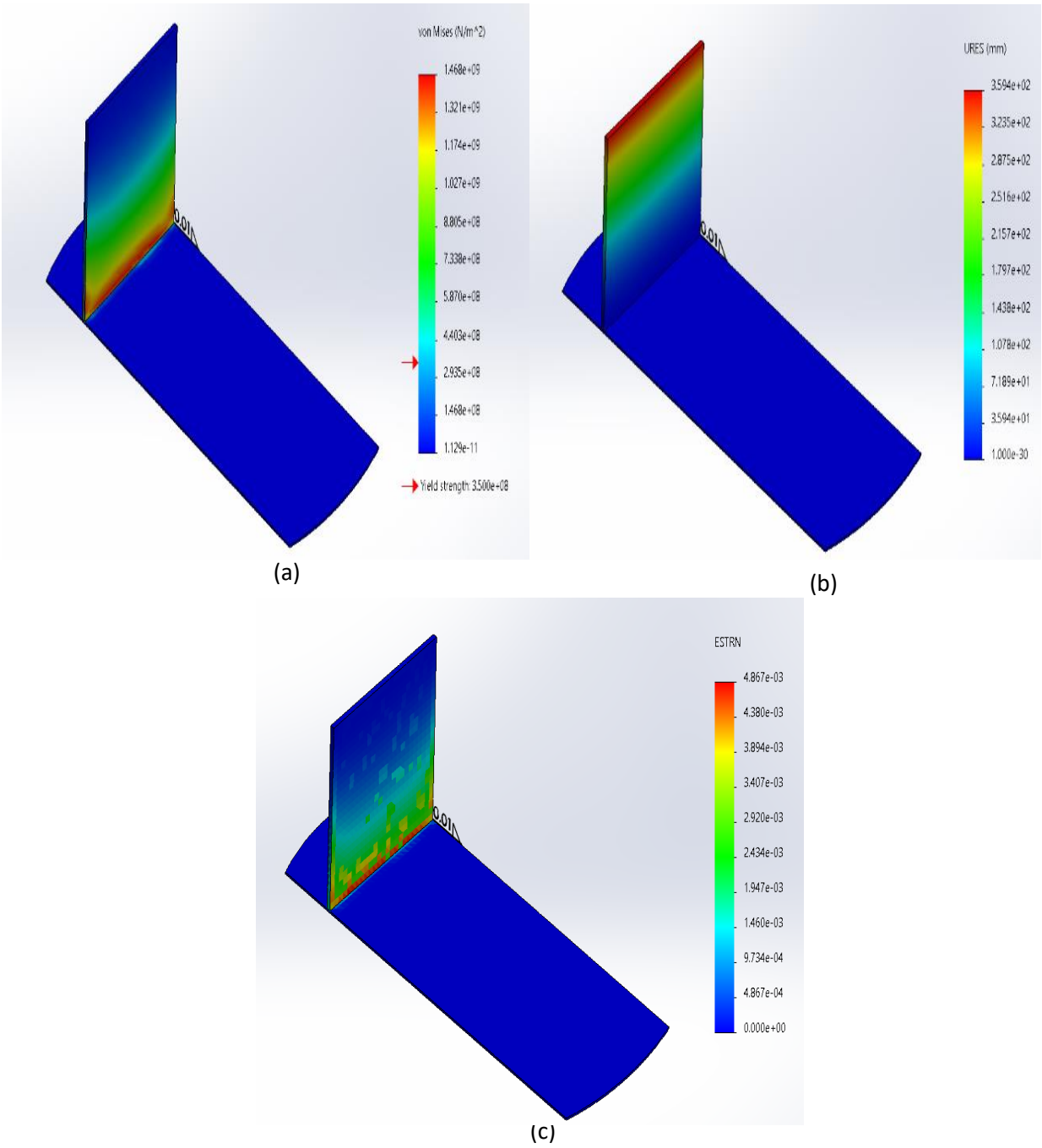

Figure 17: Results for 70mm wall AISI 1020 cold rolled steel (a) Von Mises stress (b) displacement (c) ESTRN strain

Table 8: Effect of thickness variation on the design

Wall Thickness (mm)	Material Yield Strength (N/m^2)	Mass of the wall (kg)	Stress (N/m^2)	Displacement (m)	Strain (ESTRN)
20	3.50 E 08	976	6.615 E 09	3.029	2.127 E-2
30	3.50 E 08	1464	5.311 E 09	2.314	1.708 E -2
50	3.50 E 08	2440	2.725 E 09	0.91	8.610 E -3
70	3.50 E 08	3416	1.468 E 09	0.359	4.867 E -3

The results of the analysis carried out with SolidWorks are presented in Table 8. We see that a 30 mm wall can offer reasonably good resistance, even though the factor of safety here is less than one. Since the mass of the wall must be minimized, the thickness of barrier must not be larger than 30 mm. The idea is to further strengthen the wall, therefore a reinforced wall with triangular supports has been used in the next case study.

4.2 Effect of Reinforcement of the wall

By using only two triangular supports for the barrier wall, we observe improvement in the strength of material with lesser accumulated stresses, but we see that the deformation is very large in the central part, and therefore it is a good idea to use the additional protection by using third triangular support for the wall at the center. It is also observed that stresses are accumulated in the edges at the welded points between the wall and triangular supports. The results for the simulation for two triangular supports are shown in figure 18.

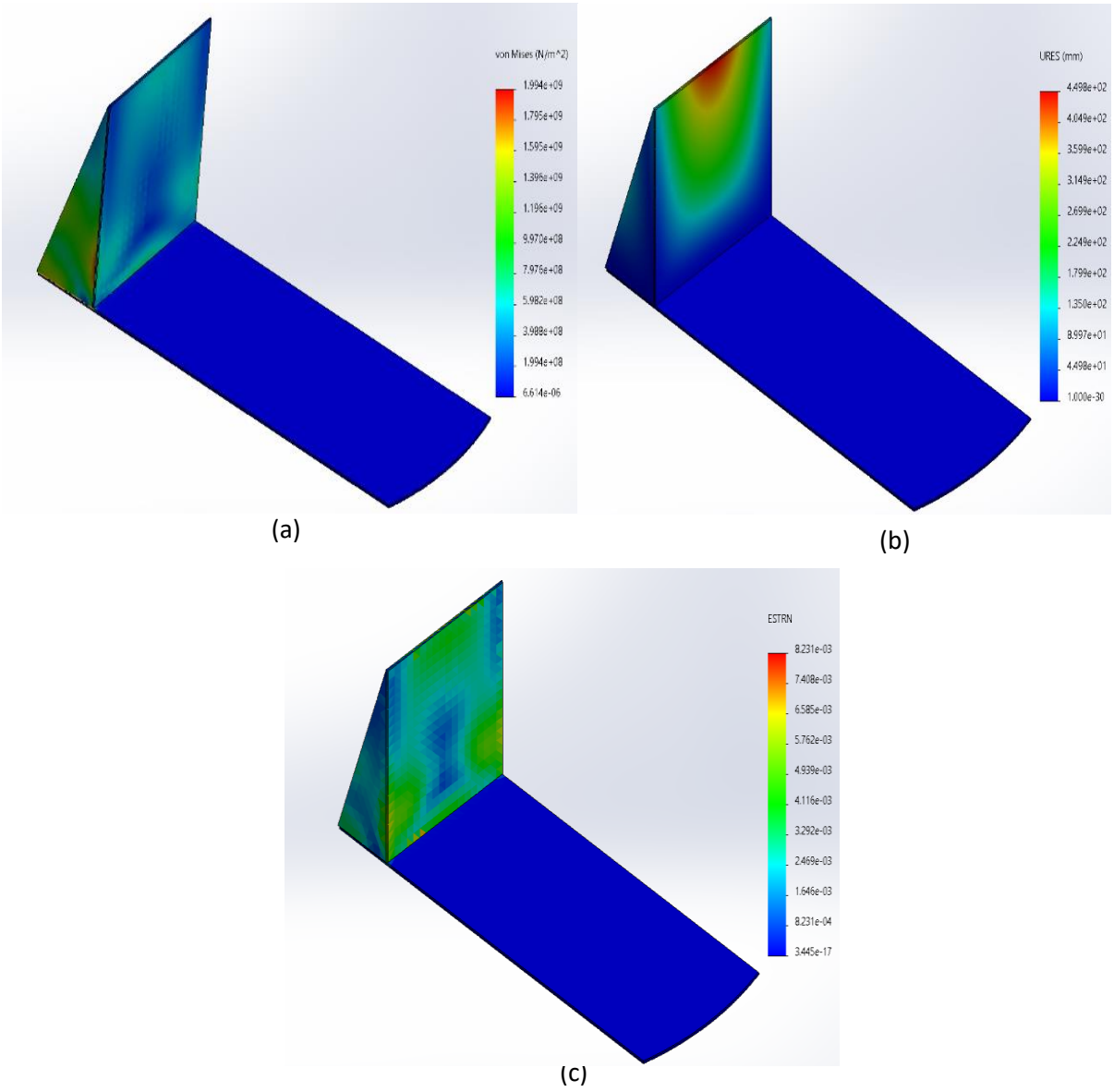

Figure 18: Results of the reinforced wall with two triangular supports (a) Von Mises stress (b) displacement (c) ESTRN strain

Figure 19 shows the analysis carried out to see the effects of further reinforcement by using three equally spaced reinforcement walls. The stress results are under the acceptable range, but we see some excessive deformations in figure 18 (b). However, with three triangular supports, we see that the reinforcement has improved the design significantly, although it comes with additional cost and weight per reinforcement incurred by using triangular support.

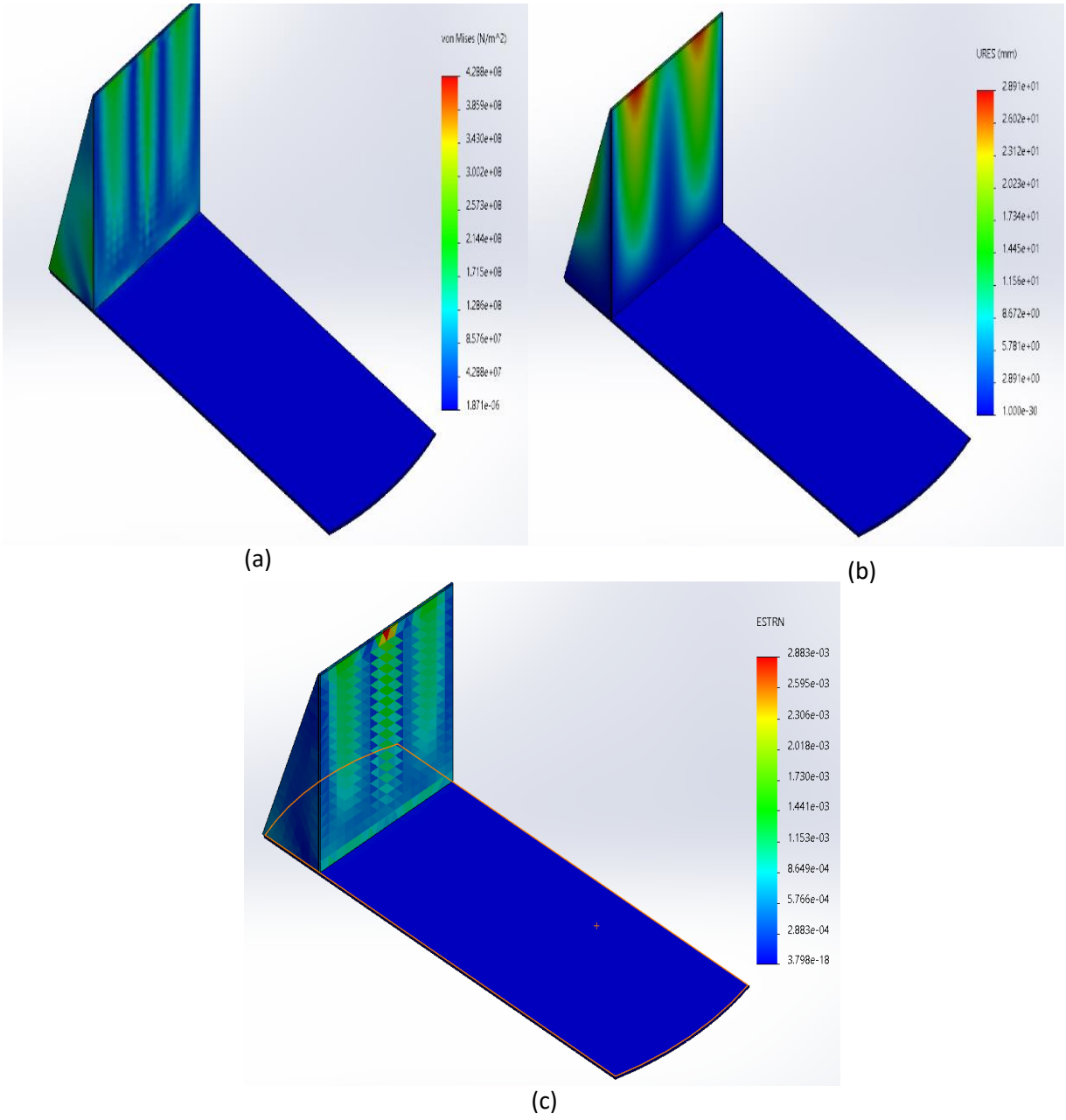

Figure 19: Results of the Reinforcement with three triangular supports to the barrier wall (a) Von Mises stress (b) displacement (c) ESTRN strain

4.3 Effect of change of shape of the safety wall with reinforcement

It is important to consider the effects on the strength of the safety wall by altering the shape of the wall. Inspired by state of the art in trailers used by (WeldshipCorporation, 2021), the effects on the design have been analyzed. It is immediately clear that the pentagonal structure helps in the saving of material. The results have been shown in figure 20. In this analysis, there are two triangular supports used to reinforce the structure.

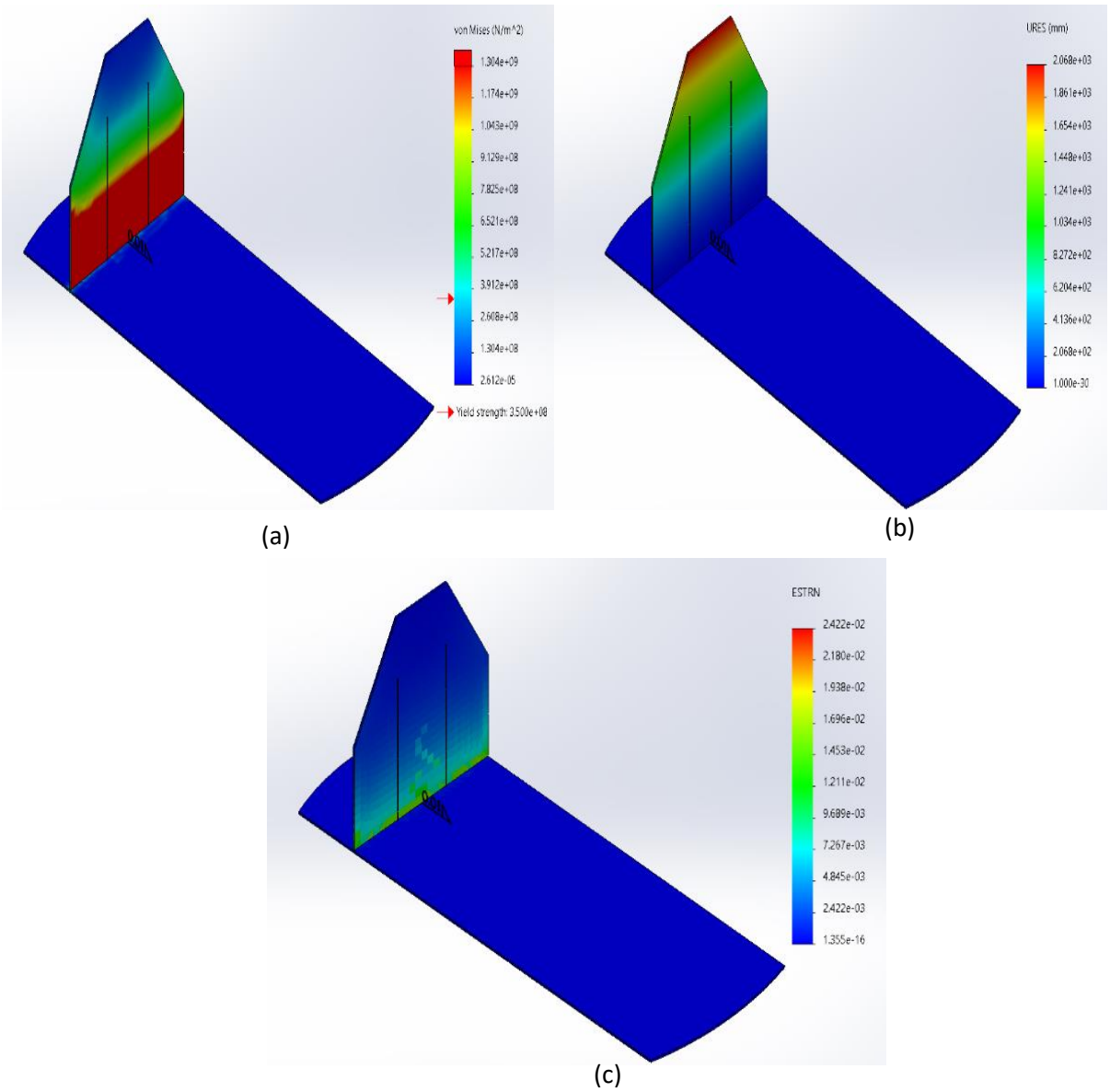

(a) (b)

(c)

Figure 20: Results of the Reinforcement with pentagonal shape on the design (a) Von Mises stress (b) displacement (c) ESTRN strain

As clear from figure 21, the displacement values seem to be extremely high, the length of the triangular supports has been increased from previously 1800 mm to 2200 mm. The effects on the results via simulation are negligibly different for the stress, but for the maximum displacement and strain, these values are found to be 0.017 m and 3.996 E -03 ESTRN. The displacements and strain contours are shown in figure 21. Von Mises stress results are not shown, as the difference in the results was negligible as compared to the analysis shown in figure 21. However, the mass per triangular support increased from the previously 158 kg to 240 kg.

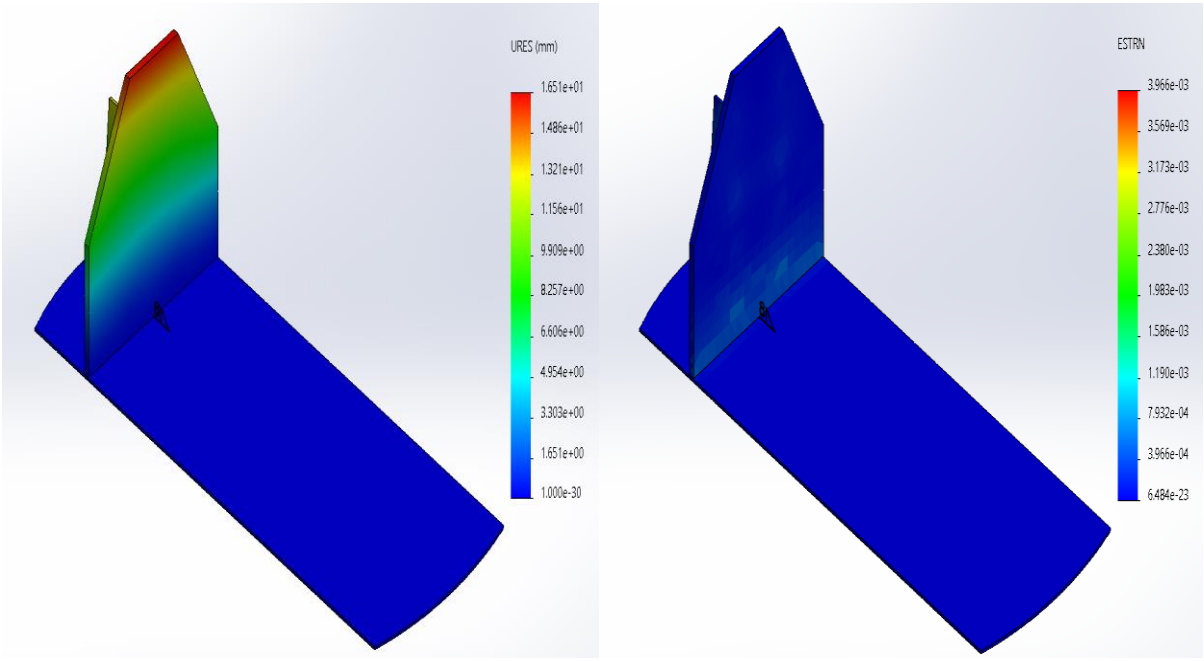

(a) (b)

Figure 21: Results of the Reinforcement with pentagonal shape with taller triangular supports on the design (a) displacement (b) ESTRN strain

Table 9 summarizes the effects of the variation of shape and reinforcements. It can be observed that the reinforcements improve the overall behavior of the material, however, there is also a significant improvement in the stress response to the pressure. The strain behavior also improves with more reinforced triangular supports. The pentagonal wall shows lesser mass and better stress and strain responses than the equivalent simple wall with two triangular supports. This design is further simulated with a thicker wall to meet the design requirements. The height of the supporting structures behind the wall remains the same as 1800 mm as was used in the previous analysis.

Table 9: Effect of reinforcement types on the design

Model Configuration Type	**Material Yield Strength (N/m^2)**	**Mass of Triangular supports (kg)**	**Mass of the wall (kg)**	**Stress (N/m^2)**	**Displacement (m)**	**Strain (ESTRN)**
Simple wall with two triangular supports	3.50E 08	305 (*2)	1464	1.994 E 09	0.449	8.231 E-3
Simple wall with three triangular supports	3.50E 08	305 (*3)	1464	4.288 E 08	0.029	2.883 E -3
Pentagonal wall with two triangular supports(1800mm)	3.50E 08	158 (*2)	1233	1.304 E 09	2.068	2.422 E -2
Pentagonal wall with two triangular supports(2200mm)	3.50E 08	240 (*2)	1233	1.304 E 09	0.017	3.996 E -03

4.4 Optimum Design (50 mm reinforced pentagonal wall)

Based on the results from the analysis carried out in the previous sections, the pentagonal wall seems to offer a good balance of low mass and high strength. However, instead of the 30 mm thickness, now 50mm thickness has been assumed and the results are posted as shown in table 10. From the stress contours, we see only blue regions indicating safe loading, whereas the factor of safety of is 2.7. The strain and displacements are almost negligible, and it is, therefore, a very safe design.

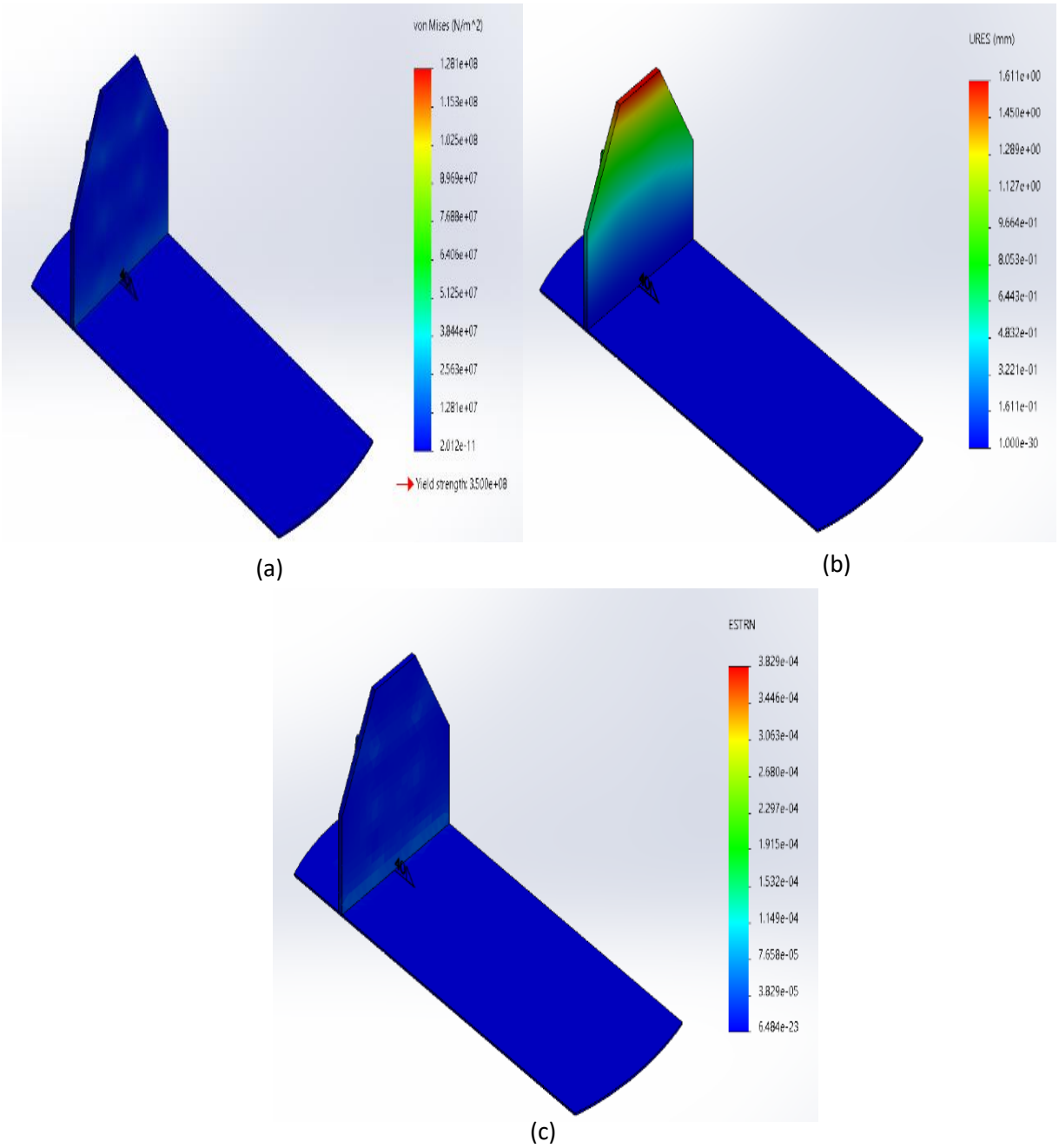

Figure 22: Results of the reinforcement with 50 mm pentagonal barrier shape on the design (a) Von Mises stress (b) displacement (c) ESTRN strain

Table 10: Optimum Design

Model Configuration Type	Material Yield Strength (N/m^2)	Mass of Triangular supports (kg)	Mass of the wall (kg)	Stress (N/m^2)	Displacement (m)	Strain (ESTRN)
Pentagonal wall with two triangular supports (50 mm)	3.50 E 08	158 (*2)	2245	1.281 E 08	0.016	3.829 E -4

5. Discussion

The main objective of the study is to propose consequences-reducing measures of safeguarding the life of CGH2 trailers' drivers. In section 2, the theoretical foundation for understanding the need for the design of a safety wall for CGH2 was established. As discussed in section 2, the loss of hydrogen containment is highly hazardous due to its hazardous properties. ISO standards and ADR regulations for hydrogen handling were briefly described. To comply with ADR regulations, the driver's cabin must be separated from the hydrogen tank by a continuous wall. In section 3.2, the risk assessment methodology was outlined the bow-tie methodology was illustrated, and the tank rupture hazards were identified. Based on the research findings of (Kashkarov et al., 2020), and (Bang et al., 2017), a safety wall between the tank and driver's cabin is necessary to reduce the impact of the blast wave. Even though six independent protection layers for mitigation of CGH2 tank explosion were listed, the focus of the study was to carry out a FEM analysis of the safety wall and propose an optimum design based on the acceptable risk level and cost. The literature review established the fact that while a lot of studies have been done on the design of safety barriers for explosions, none of them deals with the design of the safety wall between the hydrogen tank and the driver's cabin. The study is supported by the finite element analysis. The grid independence of the model was verified, and the result was satisfactory.

The second main objective of the study was to analyze the physical and mechanical properties of the safety wall and suggest additional layers of safety to the MCE AS company for the safe transportation of CGH2 in semi-trailers. The design of the safety barrier wall against the CGH2 tank explosion involved several steps which are summarized in table 7. The study considered the design of a vertical wall against the overpressure of 400 kPa through SolidWorks simulation. The initial study concluded that the model configuration and the design parameters alone would not offer complete protection against hydrogen tank explosion. The analysis gave a good understanding of the material properties and the selection of the high strength, and low weight material under the five choices considered in the study. The material AISI 1020 cold-rolled steel was deemed the safest of the options for the safety wall due to its relatively higher strength, ductility, and good weldability.

The next key parameter of the design studied was the effect of thickness of the wall. The results can be seen in table 8. The wall thickness of 20, 30, 50, and 70 mm were considered in the analysis. While the study followed the systematically increased resistance to the overpressure with the increments in thickness, the mass of the hydrogen wall appeared to be a limiting factor for the company to implement it practically. Even with the largest thickness of 70 mm, the wall barely offered full protection, as the stress value was still larger than the material yield strength. Since the mass is a critical factor, the results of the study showed that 30 mm width was the optimum option based on safety and weight factors. The reinforced barrier wall was then simulated with two and three triangular supports at the back. This design with two triangular supports significantly improved the strength of the wall, especially the strain which decreased to approximately 0.5 m from 2.3 m for the 30 mm wall thickness. The stress behavior also improved significantly. The highest stresses were found to be accumulated in the sharp edges of the wall. The study with three triangular supports further reinforced the design with better stress and strain tolerances. While the displacement came down to 0.029 m, the stress was reduced to 4.3 E 08 N/m^2. The simulation of the reinforced pentagonal wall with 30 mm width resulted in relatively higher stress and strain values, even though it offered a significant reduction in the weight of the overall reinforced structure. This analysis has been reported in table 9. The optimum design has been proposed in table 10 which uses a 50 mm reinforced pentagonal wall with two modified supports for the pentagonal wall. The structure offered a very good response to the stress and strain, and it can protect against the hydrogen tank explosion by

maintaining a factor of safety of approximately 3. This discussion has been summarized in table 10. While the pentagonal structure offered good overall resistance, it must be highlighted that the structure should fully cover the truck cabin. The mass of the wall with 50mm is a drawback with the the optimum design even though the mass is approximate 9 % lesser than the same width used for simple wall. The height of the modified triangular supports must be optimized, as section 4.3 highlighted the improvement potential of using longer reinforced walls at the cost of the mass of the structures used for reinforcing. The design shown in fig 4 (a) is based on the arrangement of the tube cylinders on the truck. The design of the safety wall covers the tube tanks completely. While the study was focused on the study of the overpressure effects of the explosion, other hazards related to CGH2 must be investigated like thermal hazards and leakage.

The final objective of the study was to provide support for the risk assessment and safety design for CGH2 storages. The proposed optimum design, in addition to one or more independent safety layers of protection like explosion suppression, containment, and flame arrestors. could safeguard against the explosion of hydrogen tanks in transportation. As the study indicated, a continuous safety wall is required by the ADR regulations The findings of this study can be a good starting point for a more detailed analysis supported by experiments.

6. Conclusion and future work

The purpose of the study was to design the safety wall as a standalone consequence-reducing measure for the high-impact explosion of the CGH2 tank. A solid foundation for highlighting the need for designing the barrier wall was developed in the background section. The aggressive nature of hydrogen to result in major accidents was reiterated from section 2 (background) of the study. The European regulations and laws related to hydrogen safety particularly in the transportation sector (ADR) were also highlighted in the same section. The study also highlighted the gaps in the legislations which are key for hydrogen to be a successful energy carrier in the future. The need for the safety wall was emphasized with examples of hydrogen accidents where the drivers were the first reported casualties. Additionally, other safety-related challenges of this promising energy carrier were also highlighted. The literature review established the fact that there is very little research to this date on the design of a safety barrier between the driver's cabin and the tank in trucks.

The results of the study provided an optimum design for the protection of the driver's cabin. The design followed the systematic procedure of selecting the safe and optimum material, thickness, and geometry.

- The most suited material for the barrier wall is AISI 1020 cold rolled steel.
- Pentagonal reinforced wall offers good resistance to overpressure and is an optimum choice as it is also relatively lighter as compared to other model configurations considered.
- The optimum design, i.e., pentagonal wall with two triangular supports offers a factor of safety of 3 and can be used without any other additional safety layers of protection.

Even though the design proved to be fully protective in case of the maximum overpressure as identified in the study, additional consequence-reducing measures have also been identified (e.g. explosion suppression, containment, and flame arrestors). This design can give a good overview to the MCE company for transporting CGH2. The findings of the study are intended to provide a holistic view about the important structural modification that must be carried out for the safe CGH2 transportation. The findings from the study illustrate the need for future work in the following areas.

- A thermal study on the same barrier wall could be carried out, and as per the findings, some additional layers for thermal protection like fire coating could be identified.
- Additional consequence reducing measures could be studied and identification of independent safety layers could result in a highly safe overall design.
- Experiments could be carried out to validate and verify the results of the FEM analysis.

References

AHLUWALIA, R., PENG, J., ROH, H., HUA, T., HOUCHINS, C. & JAMES, B. 2018. Supercritical cryo-compressed hydrogen storage for fuel cell electric buses. *International Journal of Hydrogen Energy,* 43**,** 10215-10231.

ALEIXO, L., ISTAD, M., SOLVANG, T. & NORDGÅRD, D. E. 2012. Experiences from integrating distributed generation in Norway: Results from a DSO survey 2010/2011.

ANDREASSEN, K., BUENGER, U., HENRIKSEN, N., ØYVANN, A. & ULLMANN, O. 1993. Norwegian hydro energy in Germany (NHEG). *International journal of hydrogen energy,* 18**,** 325-336.

ASHBY, M. F. & JOHNSON, K. 2013. *Materials and design: the art and science of material selection in product design*, Butterworth-Heinemann.

BALDWIN, D. 2017. Development of high pressure hydrogen storage tank for storage and gaseous truck delivery. Hexagon Lincoln LLC, Lincoln, NE (United States).

BANG, B., PARK, H., KIM, J., AL-DEYAB, S. S., YARIN, A. L. & YOON, S. S. 2017. Analytical and numerical assessments of local overpressure from hydrogen gas explosions in petrochemical plants. *Fire and materials,* 41**,** 587-597.

BARILO, N., DALTON, A. & KALLMAN, R. 2019. An investigation of mobile hydrogen and fuel cell technology applications.

BARTHELEMY, H., WEBER, M. & BARBIER, F. 2017. Hydrogen storage: recent improvements and industrial perspectives. *International Journal of Hydrogen Energy,* 42**,** 7254-7262.

BOSSEL, U. & ELIASSON, B. 2003. Energy and the hydrogen economy. *Methanol Institute, Arlington, VA*.

BRACHA, M., LORENZ, G., PATZELT, A. & WANNER, M. 1994. Large-scale hydrogen liquefaction in Germany. *International journal of hydrogen energy,* 19**,** 53-59.

BURT, V. 2015. *Corrosion in the petrochemical industry*, ASM International.

CADWALLADER, L. C. & HERRING, J. S. 1999. Safety issues with hydrogen as a vehicle fuel. Idaho National Engineering and Environmental Laboratory, Idaho Falls, ID (US).

CLEANTECH, N. M. 2019. Norwegian future value chains for liquid hydrogen. *Report. URL: https://maritimecleantech. no/wp-content/uploads/2016/11/Report-liquid-hydrogen. pdf*.

CROW, J. 2019. Hydrogen storage gets real. *Chemistry World*.

DADASHZADEH, M., KASHKAROV, S., MAKAROV, D. & MOLKOV, V. 2018. Risk assessment methodology for onboard hydrogen storage. *International Journal of Hydrogen Energy,* 43**,** 6462-6475.

DAMMAN, S., SANDBERG, E., ROSENBERG, E., PISCIELLA, P. & JOHANSEN, U. 2020. Largescale hydrogen production in Norway-possible transition pathways towards 2050. *SINTEF Rapport*.

DRIVE, U. 2017. Hydrogen Delivery Technical Team Roadmap July 2017.

EDESKUTY, F. J. & STEWART, W. F. 1996. *Safety in the handling of cryogenic fluids*, Springer Science & Business Media.

ENVIRONMENT, N. M. O. C. A. 2021. *Seas and coastlines - the need to safeguard species diversity* [Online]. Ministry of Climate and Environment. [Accessed 20 June 2021].

EU, H. 2019. Horizontal Position Paper Transport and Distribution of Compressed Hydrogen by Road Quantity and Pressure Limitations.

EUROPE, H. 2020. *Hydrogen Transport & Distribution* [Online]. Available: https://hydrogeneurope.eu/hydrogen-transport-distribution [Accessed 15 August 2020].

GEBBEKEN, N. & DÖGE, T. 2010. Explosion protection—architectural design, urban planning and landscape planning. *International Journal of Protective Structures,* 1**,** 1-21.

HEXAGONCOMPOSITES 2015. Global perspectives & Norwegian opportunities

Storage and transport of compressed hydrogen

HIRTH, J. & JOHNSON, H. 1976. Hydrogen problems in energy related technology. *Corrosion,* 32**,** 3-26.

HOUF, W. G., EVANS, G. & SCHEFER, R. 2009. Analysis of jet flames and unignited jets from unintended releases of hydrogen. *International Journal of Hydrogen Energy,* 34**,** 5961-5969.
HYLAW. 2020. *Quantity and Pressure limitation* [Online]. Available: https://www.hylaw.eu/database/norway/transport-and-distribution-of-hydrogen/road-transport-in-cylinders-and-tube-trailers-bulk-gas-metal-hydride-bulk-liquid/quantity-and-pressure-limitation [Accessed 15 August 2020].
HYWAYS, S. 2008. *Hydrogen energy in Europe, integrated project under the 6th FP of the European Commission* [Online]. Available: www.hyways.de [Accessed 2021].
IEA (2019), T. F. O. H., IEA, PARIS *The Future of Hydrogen, Seizing today's opportunities* [Online]. Available: https://www.iea.org/reports/the-future-of-hydrogen [Accessed].
ISHIMOTO, Y., VOLDSUND, M., NEKSÅ, P., ROUSSANALY, S., BERSTAD, D. & GARDARSDOTTIR, S. O. 2020. Large-scale production and transport of hydrogen from Norway to Europe and Japan: Value chain analysis and comparison of liquid hydrogen and ammonia as energy carriers. *International Journal of Hydrogen Energy,* 45**,** 32865-32883.
KASHKAROV, S., LI, Z. & MOLKOV, V. 2020. Blast wave from a hydrogen tank rupture in a fire in the open: Hazard distance nomograms. *International Journal of Hydrogen Energy,* 45**,** 2429-2446.
KELLY, M. R., SCHMID, S. R., ADAMS, D. C., FLETCHER, J. & HEARD, R. 2019. Experimental investigation of linear friction welding of AISI 1020 steel with pre-heating. *Journal of Manufacturing Processes,* 39**,** 26-39.
KIKUKAWA, S., MITSUHASHI, H. & MIYAKE, A. 2009. Risk assessment for liquid hydrogen fueling stations. *international journal of hydrogen energy,* 34**,** 1135-1141.
KUROWSKI, P. 2013. *Engineering Analysis with SolidWorks Simulation 2013*, SDC publications.
LACHANCE, J., TCHOUVELEV, A. & ENGEBO, A. 2011. Development of uniform harm criteria for use in quantitative risk analysis of the hydrogen infrastructure. *international journal of hydrogen energy,* 36**,** 2381-2388.
LAHNAOUI, A., WULF, C., HEINRICHS, H. & DALMAZZONE, D. 2018. Optimizing hydrogen transportation system for mobility by minimizing the cost of transportation via compressed gas truck in North Rhine-Westphalia. *Applied energy,* 223**,** 317-328.
MCCARTY, R. D., HORD, J. & RODER, H. M. 1981. *Selected properties of hydrogen (engineering design data)*, US Department of Commerce, National Bureau of Standards.
MCE. 2021. *MCE AS , om oss* [Online]. [Accessed 20 June 2021].
MICHEL, N., PIER PAOLO, R., ROSSANA, S. & MANFRED, H. 2021. The Role of Green and Blue Hydrogen in the Energy Transition—A Technological and Geopolitical Perspective. *Sustainability (Basel, Switzerland),* 13**,** 298.
MITAL, S. K., GYEKENYESI, J. Z., ARNOLD, S. M., SULLIVAN, R. M., MANDERSCHEID, J. M. & MURTHY, P. L. 2006. Review of current state of the art and key design issues with potential solutions for liquid hydrogen cryogenic storage tank structures for aircraft applications.
MODISHA, P. M., OUMA, C. N., GARIDZIRAI, R., WASSERSCHEID, P. & BESSARABOV, D. 2019. The prospect of hydrogen storage using liquid organic hydrogen carriers. *Energy & fuels,* 33**,** 2778-2796.
MOLKOV, V., CIRRONE, D., SHENTSOV, V., DERY, W., KIM, W. & MAKAROV, D. Blast wave and fireball after hydrogen tank rupture in a fire. 11th International Colloquium on Pulsed and Continuous Detonations, 2019. TORUS PRESS Ltd.
MOLKOV, V. & KASHKAROV, S. 2015. Blast wave from a high-pressure gas tank rupture in a fire: Stand-alone and under-vehicle hydrogen tanks. *International Journal of Hydrogen Energy,* 40**,** 12581-12603.
MOMIRLAN, M. & VEZIROGLU, T. N. 2005. The properties of hydrogen as fuel tomorrow in sustainable energy system for a cleaner planet. *International journal of hydrogen energy,* 30**,** 795-802.
NEVILLE, A. 2009. Lessons learned from a hydrogen explosion. *Power,* 153**,** 48-48.

NEWBOROUGH, M. & COOLEY, G. 2020. Developments in the global hydrogen market: The spectrum of hydrogen colours. *Fuel Cells Bulletin,* 2020**,** 16-22.
NORWEGIAN MINISTRY OF PETROLEUM AND ENERGY, N. M. O. C. A. E. 2020. *The Norwegian hydrogen strategy* [Online]. Government.no. [Accessed 20th June 2021].
ØYSTESE, K. 2019. *Ferjekontrakt viktig sted mot produksjon av flytende hydrogen i Norge, article at Energi og Klima* [Online]. [Accessed 21 Oct 2020].
PANT, K. & GUPTA, R. B. 2009. Fundamentals and use of hydrogen as a fuel. *Hydrogen fuel: production, transport, and storage***,** 3-32.
RISK, C. 2020. *BowTieXP Visual Risk Assessment* [Online]. Available: https://www.cgerisk.com/products/bowtiexp/ [Accessed Nov 11 2020].
ROACHE, P. J. 1993. A method for uniform reporting of grid refinement studies. *ASME-PUBLICATIONS-FED,* 158**,** 109-109.
ROSEN, M. A. & KOOHI-FAYEGH, S. 2016. The prospects for hydrogen as an energy carrier: an overview of hydrogen energy and hydrogen energy systems. *Energy, Ecology and Environment,* 1**,** 10-29.
ROSTRUP-NIELSEN, J. R. & ROSTRUP-NIELSEN, T. 2002. Large-scale hydrogen production. *Cattech,* 6**,** 150-159.
SIMBECK, D. & CHANG, E. 2002. Hydrogen supply: cost estimate for hydrogen pathways–scoping analysis. *National Renewable Energy Laboratory,* 71.
SOLIDWORKS, D. 2021. *Get the Facts about Simulation Accuracy* [Online]. Available: https://www.solidworks.com/media/get-facts-about-simulation-accuracy [Accessed 4th June 2021 2021].
STILLER, C., SVENSSON, A. M., MØLLER-HOLST, S., BÜNGER, U., ESPEGREN, K. A., HOLM, Ø. B. & TOMASGÅRD, A. 2008. Options for CO2-lean hydrogen export from Norway to Germany. *Energy,* 33**,** 1623-1633.
TEMPLIER, M. & PARÉ, G. 2015. A framework for guiding and evaluating literature reviews. *Communications of the Association for Information Systems,* 37**,** 6.
USTOLIN, F., PALTRINIERI, N. & BERTO, F. 2020. Loss of integrity of hydrogen technologies: A critical review. *International Journal of Hydrogen Energy*.
VEZIRO, T. & BARBIR, F. 1992. Hydrogen: the wonder fuel. *International Journal of Hydrogen Energy,* 17**,** 391-404.
WELDSHIPCORPORATION. 2021. *Super max Jumbo Hydrogen tube trailer* [Online]. WeldshipCorporation. Available: http://www.weldship.com/about-us/super-max-hydrogen-jumbo-tube-trailer.html [Accessed 28 May 2021 2021].
WIJAYANTA, A. T., ODA, T., PURNOMO, C. W., KASHIWAGI, T. & AZIZ, M. 2019. Liquid hydrogen, methylcyclohexane, and ammonia as potential hydrogen storage: Comparison review. *International Journal of Hydrogen Energy,* 44**,** 15026-15044.
WILLOUGHBY, D. & ROYLE, M. 2011. The interaction of hydrogen jet releases with walls and barriers. *International journal of hydrogen energy,* 36**,** 2455-2461.
XU, B. P. & WEN, J. X. 2012. Numerical study of spontaneous ignition in pressurized hydrogen release through a length of tube with local contraction. *International Journal of Hydrogen Energy,* 37**,** 17571-17579.
YANG, C. & OGDEN, J. 2007. Determining the lowest-cost hydrogen delivery mode. *International Journal of Hydrogen Energy,* 32**,** 268-286.
ZENG, K. & ZHANG, D. 2010. Recent progress in alkaline water electrolysis for hydrogen production and applications. *Progress in energy and combustion science,* 36**,** 307-326.
ZHIYONG, L., XIANGMIN, P. & JIANXIN, M. 2010. Harm effect distances evaluation of severe accidents for gaseous hydrogen refueling station. *International journal of hydrogen energy,* 35**,** 1515-1521.
ZOHURI, B. 2019. Hydrogen Energy : Challenges and Solutions for a Cleaner Future. 1st ed. 2019. ed. Cham: Springer International Publishing : Imprint: Springer.

Appendix

Appendix A:

A.1 Tank Specification provided by MCE AS.

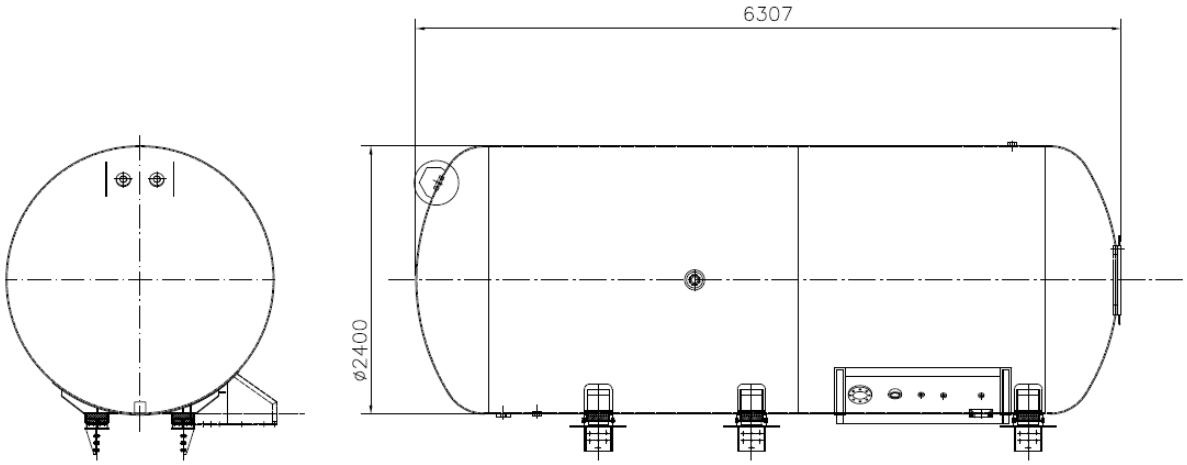

A.2 Material Properties (The values are taken from SolidWorks 2020)

Material Property	Value	Units
Yield Strength	3.50E+09	N/m^2
Thermal Conductivity	5.19E+01	W/(m.K)
Mass Density	7.87E+03	kg/m^3
Coefficient of thermal expansion	1.17 * 10^-5	/K
Specific heat	4.86E+02	j/(kg.K)
AISI 1020 Steel, Cold Rolled		

Material Property	Value	Units
Yield Strength	1.80E+09	N/m^2
Thermal Conductivity	5.19E+01	W/(m.K)
Mass Density	7.87E+03	kg/m^3
Coefficient of thermal expansion	1.22 * 10^-5	/K
Specific heat	4.48E+02	j/(kg.K)
AISI 1010 Steel, Hot Rolled		

Material Property	Value	Units
Yield Strength	2.21E+08	N/m^2
Thermal Conductivity	4.30E+01	W/(m.K)
Mass Density	7.80E+03	kg/m^3
Coefficient of thermal expansion	1.3 * 10^-5	/K
Specific heat	4.40E+02	j/(kg.K)
Plain Carbon Steel		

Material Property	Value	Units
Yield Strength	2.76E+08	N/m^2
Thermal Conductivity	2.20E+02	W/(m.K)
Mass Density	2.70E+03	kg/m^3
Coefficient of thermal expansion	2.4 * 10^-5	/K
Specific heat	1.00E+03	j/(kg.K)
1345 Aluminium Alloy		

Material Property	Value	Units
Yield Strength	7.10E+08	N/m^2
Thermal Conductivity	4.45E+01	W/(m.K)
Mass Density	7.85E+03	kg/m^3
Coefficient of thermal expansion	1.23 * 10^-5	/K
Specific heat	4.75E+02	j/(kg.K)
AISI 4340 Steel, Normalized		

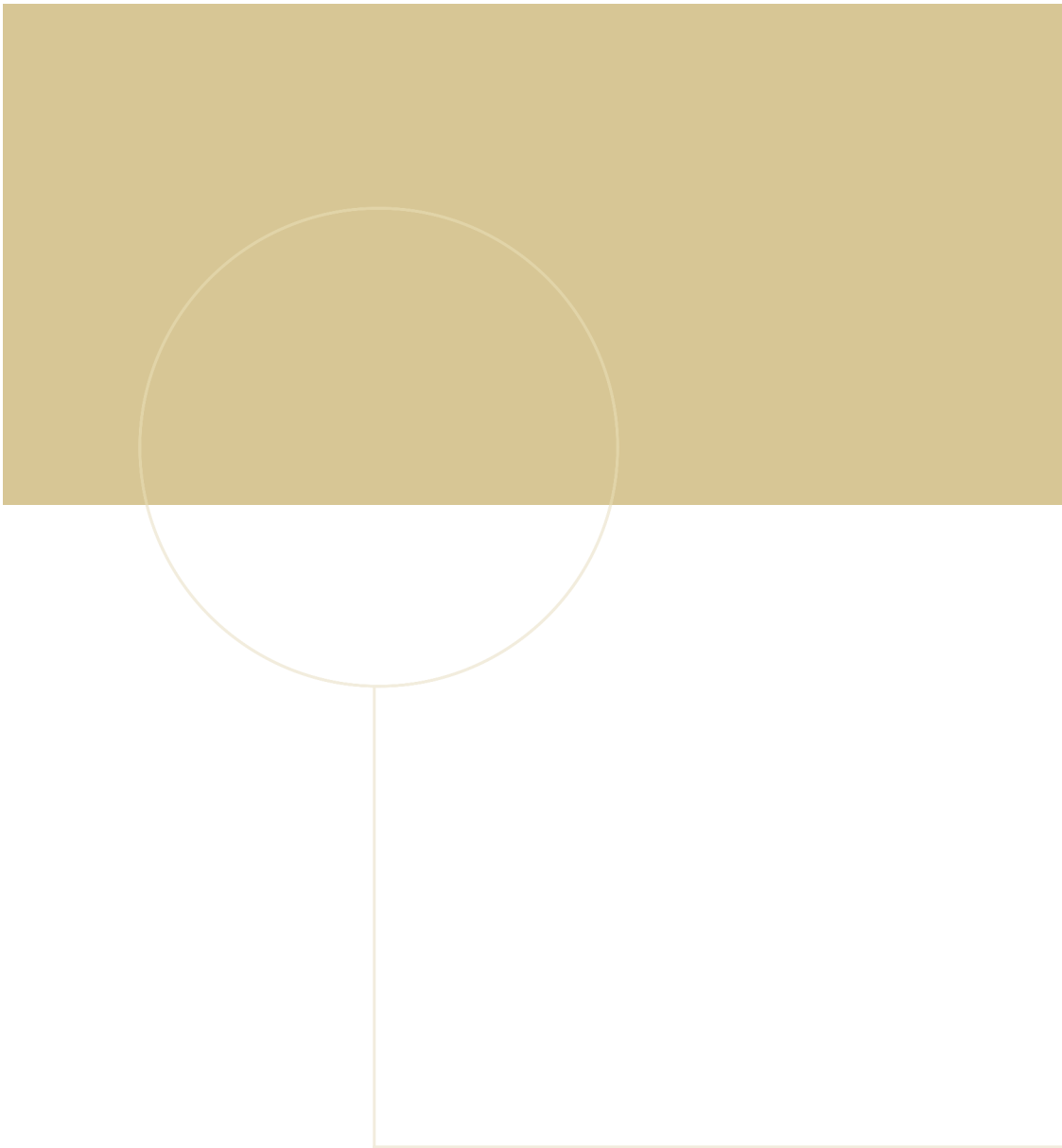

NTNU

Norwegian University of
Science and Technology